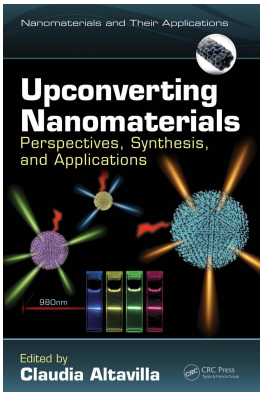

Upconverting Nanomaterials Perspectives, Synthesis, and Applications

Claudia Altavilla

Upconversion Nanoparticles for Phototherapy

Publication details
https://test.routledgehandbooks.com/doi/10.1201/9781315371535-12
Akshaya Bansal, Zhang Yong
Published online on: 10 Oct 2016

9

Upconversion Nanoparticles for Phototherapy

Akshaya Bansal and Zhang Yong

CONTENTS

9.1 Introduction: Need for NIR-Based Phototherapy

Photoactivation has garnered tremendous interest in the last decade, with widespread applications ranging from medicine to energy harvesting and even wastewater treatment. This increasing interest stems from the fact that photoactivation allows the use of light—a noninvasive, spatially, and temporally controllable stimulus to achieve specific outcomes. This is particularly useful for therapeutic applications where specificity and safety are a major concern. With the use of light, therapy can be targeted, reducing side effects and improving efficacy of treatment. In addition, the ability to control

parameters such as wavelength, intensity, and duration of exposure, provide an added degree of control. To this end, phototherapies such as photodynamic therapy (PDT), photothermal therapy (PTT), photocontrolled release of drugs/nucleic acids, and combination therapies involving synergistic use of two or more of the previous techniques have come to the fore.

PDT involves the use of photoresponsive chemicals called photosensitizers (PSs), which produce reactive oxygen species (ROS) upon irradiation with light of a particular wavelength (usually in the visible range), subsequently killing cells in the vicinity. This type of targeted cell kill is being explored as a cancer-treatment modality. Besides PDT, localized generation of ROS at lower concentrations is also used to improve cytoplasmic delivery of biomolecules into cells, a technique called photochemical internalization (PCI). In PCI, the amount of ROS generated is not enough to kill the cell but can rupture endosomes into which the cells take up biomolecules of interest through endocytosis. This causes the cargo to be released into the cytoplasm. Besides generation of ROS, there are phototherapies working on different principles such as light to heat transduction, as is the case with PTT. Localized increase in temperature can also be used to kill cells in a targeted manner and is being developed as a cancer therapy. In addition to the phototherapies mentioned above, light can also be used for controlled delivery of biomolecules. This is usually done by either "caging" the molecule of interest or sequestering it through the use of photolabile moieties. Upon irradiation with light of a suitable wavelength (usually ultraviolet [UV] light), the caging or sequestering photolabile group is cleaved, thereby "uncaging" or releasing the biomolecule of interest at the desired site. This strategy has been used for site-specific activation/delivery of chemotherapeutic drugs, nucleic acids like siRNA, and other small molecules, with greater temporal control and reduced off target effects.

Although the techniques mentioned above have great therapeutic potential, their practical applications are hindered by certain constraints. Most photoresponsive moieties used in the techniques mentioned earlier, respond either to visible or UV light. These wavelengths have low tissue penetration and UV in particular is known to be toxic. In the near-infrared (NIR) range, light absorption and tissue scattering is minimal, allowing for greater tissue penetration. Thus, phototherapies that allow use of NIR light as opposed to visible or UV light would be advantageous. Even though efforts have been made to develop NIR light sensitive moieties for use in phototherapy, the field still in its infancy. Since most photoresponsive moieties cannot use NIR light directly, a means of transducing this light to the usable visible or UV regions is needed. Upconversion nanoparticles (UCNPs) are such transducers. They are excited by light in the NIR range (most commonly 980 nm) and can be tuned to emit in the UV, visible, and infrared ranges, in accordance with the absorption requirements of the photoresponsive moiety being used. The details on how UCNPs work and their synthesis can be found in the previous chapters. This chapter will delve into the applications of UCNPs

for phototherapy, the limitations of using UCNPs, and efforts being made to overcome these limitations.

9.2 Photoinduced ROS Production

Chemicals called PSs produce ROS when irradiated with light of a suitable wavelength. This ROS production can be used therapeutically in different ways. It can be used to cause targeted cell kill in a technique called PDT or when generated in a localized manner at a lower concentration, be used to aid endosomal escape—a major bottleneck in delivery of biomolecules especially when using nanoparticles as carriers. This is called PCI (Berg et al. 2006). This section will describe both PDT and PCI in detail and explain how UCNPs are useful as both carriers and transducers, allowing the use of NIR instead of UV or visible light for these techniques, thereby improving their clinical potential.

9.2.1 Photodynamic Therapy

PDT involves dye-sensitized photooxidation of biological matter. When a photosensitizing agent is irradiated with light of a specific wavelength, oxygenated products (ROS) harmful to cell function arise, which eventually result in tissue destruction through a variety of mechanisms (Henderson and Dougherty 1992). There are three components essential for implementing PDT—a PS, light, and the presence of oxygen. Light of a suitable wavelength that matches the absorption maximum of the PS excites the electrons of this PS to a higher energy level, converting it to a short-lived singlet state and then through intersystem crossing to a relatively long-lived triplet state (Juzeniene et al. 2007). This excited state can transfer energy to a neighboring substrate, producing free radical species, which then react with the surrounding oxygen to generate superoxide anion radicals, hydroxyl radicals, and hydrogen peroxide. This type of ROS generation is classified as type I. Another mechanism, involves direct transfer of energy from a triplet-state PS to surrounding molecular oxygen resulting in the formation of singlet oxygen ($^1O_2$). This type II reaction is the prevailing mechanism of ROS generation for most PSs (Bonnett 1995; Idris et al. 2015) (Figure 9.1).

Successful application of PDT involves consideration of parameters such as PS type, its administration and distribution in the body, type of light source used, mode of light delivery, and finally the immediate and late effects of PDT. The tumoricidal effect of PDT is multifactorial and results from a variety of direct and indirect responses of the cells, vasculature, and immune system. The acute or lethal tumor cell killing effect arises from apoptosis or necrosis that results from direct damage to proteins, lipids, or nucleic acids in the

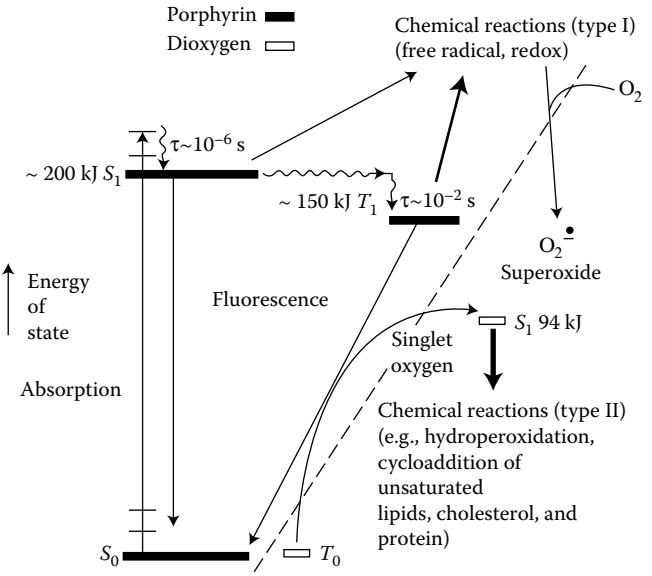

FIGURE 9.1
Schematic showing types I and II reactions for ROS generation. (Reproduced with permission from Bonnett, R., *Chem. Soc. Rev.*, 24 (1), 19–33, 1995.)

cells due to the ROS produced by the PS taken up by these cells or through oxygen and nutrient deprivation resulting from destruction of tumor vasculature. Secondary tumor killing responses on the other hand are caused due to activation of the immune system. Nonlethal photooxidative lesions of membrane lipids activate membranous phospholipidases leading to accelerated phospholipid degradation, release of lipid fragments, and metabolites of arachidonic acid that are powerful inflammatory mediators. In addition, even minor photodamage to the vasculature can attract circulating immune cells such as neutrophils and platelets, resulting in a progressive impairment of vascular function along with massive release of inflammatory cytokines. Thus, nonlethal photooxidation can set of a cascade of events leading to a strong inflammatory response further amplifying PDT-mediated tumoricidal response (Castano et al. 2006; Dougherty et al. 1998; Plaetzer et al. 2009).

The irreversible damage caused to the tissue during PDT has been used successfully for treating a variety of solid tumors such as those involving the lung, bladder, prostrate, skin, etc. Besides cancer therapy, PDT is also being explored as an antimicrobial tool with potential applications in treating infections, cardiovascular, dermatological, and ophthalmic diseases. Although promising, the widespread acceptance of PDT as a primary therapy faces certain hurdles. The most prominent of these, as mentioned earlier is the low penetration depth of light sources used. Most PSs used for PDT have an absorption maximum in the visible region of light, where tissue

absorption and scattering is high and as such light can only penetrate to a few millimeters (1–3 mm). This limits the application of PDT to superficial tumors or those accessible by an endoscope. In the 700–1000 nm range, maximal tissue transparency is attained wherein scattering and absorption of light by biomolecules is minimal. Thus, to target deeper tumors, a longer wavelength of light such as NIR is desirable. Although efforts have been made to develop PSs that respond to this range of light, the field is still in its infancy and such PSs are rare. UCNPs provide an elegant solution to this problem, wherein the older tried and tested PSs can be used in conjunction with NIR excitation. Here, these UCNPs serve as nanotransducers that convert NIR light into the visible light needed for exciting the PSs. Besides their role as transducers, these nanoparticles can also serve as carriers of these PSs and can be targeted to specific tissues through various surface modifications. The following section will delve into the various PSs used for PDT, types of UCNPs that can be used in this technique, various surface modifications that allow loading of different types of PSs on to UCNPs, targeting moieties for selective accumulation in tumor regions, and finally how such systems can be implemented *in vitro* and *in vivo*.

9.2.1.1 PSs for PDT

PSs are the central component of the light–PS–oxygen system needed for PDT. Ideally, a PS used for cancer therapy should localize preferentially to the tumor region and not accumulate in off target organs such as the lungs or the skin (unless these are desired targets), be amphiphilic so as to allow blood transport (hydrophilicity) as well as uptake by cells (lipophilicity), have low dark toxicity such that it only causes cell kill when irradiated with light, good ROS production efficiency, a high absorption coefficient at longer wavelength of light so deeper tissues can be targeted, and lastly, be easy to synthesize. In short, an ideal PS should localize to the site of interest and kill cells only when excited with light of a suitable wavelength for a targeted therapy while mitigating unwanted side effects. With these considerations in mind, several PSs have been designed for PDT. Depending on their chemical composition, they can be classified as porphyrins, chlorins, 5-aminolevulinic acid (ALA), and naphthalocyanines. Of these PSs, porphyrins are the oldest and most widely studied, with many of this family approved for clinical use. Besides porphyrins, some chlorins and phthalocyanines are also available clinically. The PSs mentioned here differ from each other in terms of circulation times, localization in specific subcellular compartments, and the wavelength of light they absorb. Some PSs like Photofrin® (a hematoporphyrin derivative) have long-circulation times while others accumulate rapidly in tissues. Rapid accumulation and clearance may be advantageous for a single application of PS followed by treatment the same day. On the other hand, long-circulation times and low clearance may allow for multiple PDT sessions with a single infusion of the PS (Allison and Sibata 2010). In addition,

those PSs with high circulation times can also be used to induce vascular shutdown following illumination and cut down of oxygen supply to the tumor, another means of bringing about tumor destruction.

A useful way to classify PSs can also be on the basis of the subcellular compartment to which they localize once the cell takes them up since the mechanism of cell lethality via PDT depends to some extent on the location of the PS in the cell. Sensitizers that tend to localize in the mitochondria like Photofrin or ALA (which produces the active compound protoporphyrin IX (PPIX) in the mitochondria), kill the cells usually through apoptosis while those that accumulate in the plasma membrane do so through necrosis in most cases (Dougherty et al. 1998). An association between mitochondrial damage due to PDT and apoptosis has been established with the release of cytochrome c and other mitochondrial factors following photodamage triggering an apoptotic reaction (Liu et al. 1996). However, use of carriers for delivering PSs can be used to significantly alter the circulation times and localization site. Details of UCNPs as carriers will be discussed in the next section.

In terms of the excitation wavelength for these PSs, the absorption maxima is usually in the visible region of light ranging from blue light around 400 nm to the red region around 650 nm. Tissue absorption and scattering increases with decreasing light wavelength, thus, the achievable tissue penetration across the visible range varies from 1 to 5 mm (approximately). Longer wavelength excitation is preferred, since it allows treatment of deeper regions in the body. Photofrin, one of the earliest developed PSs for PDT is an inefficient producer of singlet oxygen at 630 nm. In addition to 630 nm, it can also absorb at 408 and 510 nm with better ROS production efficiency (Bernstein et al. 1999). Some of its drawbacks include long-circulation times, low clearance, and accumulation in the skin, which can result in prolonged undesirable photosensitivity. However, with dose adjustments, these side effects can be minimized (Allison and Sibata 2008). ALA, a prodrug is enzymatically converted to the active form PPIX *in vivo*, which is subsequently converted to heme. This PS can also be excited using blue (410 nm), green (510 nm), or red (635 nm) wavelengths, with ROS production efficiency being highest at the shorter wavelengths (Peng et al. 1997). The phthalocyanine dye family along with its relative, the naphthalocyanines, are potent PSs for PDT-based applications. They have a porphyrin-based structure with a central atom usually of aluminum, zinc, or silicon to increase the production of singlet oxygen. Unlike the previous PSs, they have a strong absorption band in the 670 nm range and thus potential for treating relatively deeper seated tissues with lower irradiation power densities (Allen et al. 2001; Ben-Hur and Rosenthal 1985).

Although efforts have been made toward the development of PSs for PDT applications keeping in mind the ideal requirements of selectivity, amphiphilicity, long-wavelength excitation, and high ROS production efficiency, many of them only partially meet these considerations. Several of these PSs are fraught with one or more of the following undesirable characteristics

ranging from aggregation in aqueous solutions due to hydrophobic nature, poor selectivity, low extinction coefficients, absorption at relatively short wavelengths, to high accumulation rates in the skin leading to normal tissue toxicity from unintentional sunlight exposure (Idris et al. 2015). This is particularly deleterious for PSs that can persist in the system for weeks. Prolonged photosensitivity especially in the skin will render treatment painful and mar acceptance of treatment by the end users, the patients (Allison and Sibata 2010). Development of nanocarriers for delivering these PSs has come a long way in overcoming a majority of these issues. UCNPs are particularly useful in this regard, as they not only serve as carriers, but also nanotransducers allowing the use of deeper tissue penetrating NIR light for excitation of PSs. Furthermore, by coating these particles with different moieties, targeted delivery to tumor specific regions can be achieved, providing a one stop solution to the multiple problems that plague PDT at present. The following section will describe in detail how different UCNPs can be used in the delivery of different types of PSs, the various surface coatings that allow loading of PSs and preparation of aqueous formulations as well as strategies for targeting these UCNP-PS formulations to desired sites in the body.

9.2.1.2 UCNPs for PDT: Host Matrix, Dopants, and Surface Coatings

A UCNP-based PDT system consists of two main components: the nanoparticles themselves, serving as both carriers and transducers and a conduit for generating ROS, the PS. To enable the UCNPs to carry these PSs, different types of surface coatings are required depending on the nature of the PS. In addition to allowing loading of cargo, these coatings also serve to impart biofunctionality and aqueous solubility needed for formulations meant for biological use. Besides the PSs described in the previous section, some surface coatings of the UCNPs (such as titanium oxide) themselves can produce ROS via upconverted light produced by the UCNPs. In short, when using UCNPs for PDT (Hou et al. 2015; Idris et al. 2014), either conventional PSs can be loaded onto UCNPs with appropriate surface coatings or the surface coating of the UCNPs themselves could be such that it produces the required ROS required for PDT.

When using UCNPs for PDT, the first step is to choose the right type of nanoparticle, in terms of the host matrix and dopant types used. This will determine the luminescence efficiency as well as emission wavelength, both factors essential for successful implementation of PDT. The emission wavelength the nanoparticle selects should match as closely as possible to the PS being used. This will ensure that the ROS production and thus the therapeutic effect is optimal. Of the various UCNP host matrix materials, hexagonal phase $NaYF_4$ is the most popular for use in PDT. This is not surprising since it is reported to be one of the most efficient upconversion host materials (Aebischer et al. 2006). Other than $NaYF_4$, materials like $NaGdF_4$ (Qiao et al. 2012; Zhao et al. 2012), $NaLuF_4$ (Ouyang et al. 2014), and $NaYbF_4$ (S. Jin et al.

2013), have also been reported but to a lesser extent. In addition to the choice of the host material, the geometric shape of the synthesized nanoparticles also affects the luminescence efficiency, with hexagonal phase nanocrystals displaying a remarkably higher upconversion luminescence than cubic-phase ones (Liu et al. 2011).

These host matrices are doped with sensitizers and activator ions that determine the emission wavelength upon excitation with NIR light (usually 980 nm for the host materials mentioned above). The most commonly used sensitizer is Yb^{3+} (absorbs 980 nm), while the activator ions used are usually Er^{3+} and Tm^{3+}. Yb^{3+}/Er^{3+} doped particles emit mostly red and green light and are thus the UCNPs of choice for most PSs (Krämer et al. 2004). For PSs such as titanium dioxide (TiO_2) and hypocrellin A that do not absorb green or red light, and have maximal absorption in the UV and/or blue light range, UCNPs doped with Yb^{3+}/Tm^{3+} can be recruited instead (Idris et al. 2014). Core–shell UCNPs consisting of a $NaYF_4$ Yb^{3+}/Er^{3+} core coated with a $NaYF_4$ Yb^{3+}/Tm^{3+} shell or vice versa can also be synthesized (X. Liu et al. 2013). These nanoparticles would have multiple emission peaks that can be used for PS activation in conjunction with other functions such as bioimaging. Aside from the activator ions mentioned above, ions such as Gd^{3+} and Mn^{2+} can also be doped in to the host matrix. Such ions improve the luminescence efficiency while imparting paramagnetic properties to the UCNPs, allowing them to double up as a T_1- or T_2-weighted magnetic resonance imaging (MRI) contrast agents (Ni et al. 2014; C. Wang et al. 2014). From the above discussion on choice of host matrix and dopants, it can be seen that these factors are paramount toward the eventual functionality of the UCNPs and must be chosen in accordance with the end requirements of the UCNP–PDT system.

After having selected the right UCNPs matched to the PS, the next step in the UCNP-mediated PDT system is to coat these particles with a suitable material that allows the PS to be loaded on to them and confers properties amenable for biological use such as aqueous solubility, low immunogenicity, and biofunctionality (for conjugation of targeting moieties, co-therapeutic molecules, etc.). There are numerous materials used to coat UCNPs ranging from polymers such as polyethylene glycol (PEG) to ceramics such as silica (Chatterjee et al. 2010). Of these materials, polymers are by far the most popular when it comes to UCNP-based PDT. One of their most attractive features is their ability to confer stability to colloidal UCNPs in aqueous solutions, a property that is crucial to allow for deliverability in biological systems (Idris et al. 2012). Although polymers such as polyethyleneimine, PEG, polyacrylic acid (PAA), and various block copolymers of PEG, polylactic acid, etc. have been reported as surface coatings for UCNPs, PEG stands out as an attractive candidate. Besides making UCNPs water dispersible, it is enormously useful as a linker for conjugating UCNPs to targeting moieties, other drugs, etc. In addition, it has low toxicity and immunogenicity, making it suitable for *in vivo* use. Polymers like polyethyleneimine (PEI) though imparting aqueous solubility are cationic and have the disadvantage of being toxic, thus limiting

their practical use. Besides the synthetic polymers outlined above, a natural polymer-chitosan, has emerged as a viable candidate for coating these nanoparticles. Aside from its properties of biodegradability, low toxicity, and immunogenicity, its amphiphilic nature provides the addition benefit of allowing hydrophobic PSs to be loaded onto the UCNPs while providing aqueous solubility (Cui et al. 2012a,b; Zhou et al. 2012).

Ceramic coatings such as silica are also popular with one of the first papers reporting UCNP-based PDT making use of this material (Qian et al. 2009; Zhang et al. 2007). Silica coating also provides stability in aqueous solutions and has low toxicity. Usually, the PS is deposited on the UCNP surface along with the silica such that it is encapsulated in the coating, with the oxygen and ROS molecules diffusing through its pores. In addition to silica coating, mesoporous silica can also be used. Here, the pore size can be controlled in the nanometer range, allowing molecules such as PSs to be loaded onto the surface of the particles through absorption alone (Idris et al. 2012). Moreover, multiple types of moieties can be co-loaded making this is an easy yet effective delivery system.

There are advantages and disadvantages to using either one of the materials described above. Polymer coatings though attractive in terms of safety and ease of modification, are known to quench upconversion fluorescence by 50% or more, with a greater quenching seen with increasing polymer concentration (Ungun et al. 2009). Silica coatings though less prone to do so are riddled with their own drawbacks. Even though physical absorption is an easy means of loading the cargo onto the particles, it reduces the degree of control one has in terms of the release characteristics of the cargo in a biological environment.

Before moving on to means of loading of PS onto UCNPs, it is prudent to first discuss the targeting moieties alluded to in the previous sections. As mentioned earlier, it is important to be able to deliver the PS to the right site for effective treatment. Although enhanced permeability and retention (EPR) effect, is effective in directing systemically delivered agents in a greater quantity to the tumor site, at times there is not sufficient accumulation for optimal therapeutic efficacy. When using nanoparticles as carriers, an effective targeting strategy is to coat them with certain groups that specifically interact with the cell type of interest. One of the most widely used targeting moieties is folic acid (FA). FA is relatively inexpensive, stable over a wide range of pH and temperature, and has high affinity for folate receptors often overexpressed in many human cancers. Cell lines such as human choriocarcinoma (JAR) cells, murine, S180 sarcoma tumors, HeLa human cervical cancer cells, B16F0 murine melanoma cells, Bel-7402 human hepatocellular carcinoma cells, and HT29 human colon cancer cells are reported to overexpress folate receptor (Idris et al. 2015). Thus, conjugating FA to UCNPs carrying the PSs, allows for an enhanced uptake by cancer cells (Cui et al. 2012b; Idris et al. 2012; Liu et al. 2012; X. Liu et al. 2013). Another receptor overexpressed in many cancers is cluster determinant 44. Targeting moieties

such as hyaluronic acid have been used to target this receptor (Xu Wang et al. 2014). Besides these ubiquitous approaches, antibodies against proteins specific to a particular type of cancer can also be deployed. This is an effective targeting approach, albeit a more expensive one. Aptamers are relatively young players in this field but advantages such as ease of synthesis, flexibility in design, and chemical stability make them strong contenders (Tan et al. 2013). Furthermore, they have the natural ability to fold into G-quadruplex structures that can be stabilized by small-molecule ligands like porphyrin, providing a convenient means of loading porphyrin-based PSs in addition to their targeting ability (Shieh et al. 2010).

9.2.1.3 PS Loading Strategies

A key step in the UCNP-based PDT system is the loading of the PS onto the nanoparticle. Depending on the surface coating deployed, this can be done either through encapsulation, physical adsorption, or covalent linkage. Before going into details about these strategies, it is of importance to note some of the criteria for optimal PS loading. First, the loading strategy should allow for a high loading capacity so that a sufficient amount of PS is available for PDT. Second, it should permit good energy transfer between the UCNP core and PS. If the PS is encapsulated or trapped within a matrix, the matrix should allow oxygen and ROS to diffuse freely to the surrounding area. Lastly, there should be minimal leakage or premature release of PS, especially in case of systemic delivery (Idris et al. 2015).

The first strategy, encapsulation is one of the oldest. In this approach, the PS is not present on the surface of the particles or covalently linked to it, but is rather encapsulated in a matrix that coats the UCNPs or trapped between the UCNP core and surface via coatings such as lipids, polymers, etc. One of the first reports of UCNP-based PDT used encapsulation as a means of loading the PS on to the particles. The PS was trapped in a dense silica matrix achieved by mixing the PS in the reaction mixture while carrying out the silica coating process (Zhang et al. 2007). The amount of PS and thickness of the silica layer could be adjusted. Although a fast and relatively simple technique, efficient loading can only be achieved for cationic hydrophilic PSs owing to the negatively charged and hydrophilic nature of the silica matrix. This method also faces some challenges in terms of the ease of diffusion of ROS and oxygen through the matrix, which could impede the efficacy of this approach. Encapsulation-based loading has also been achieved using polymers and lipids. As mentioned earlier, chitosan is amphiphilic and provides dual advantages of loading hydrophobic PSs while presenting a hydrophilic surface for aqueous solubility. To this end, interactions between the hydrophobic part of this polymer and hydrophobic PS (such as zinc phthalocyanine (ZnPc)) have been used to trap the PS between the UCNP core and the hydrophilic part of chitosan present on the outer surface (Cui et al. 2012a,b) (Figure 9.2a). In another approach, both UCNPs and the PS

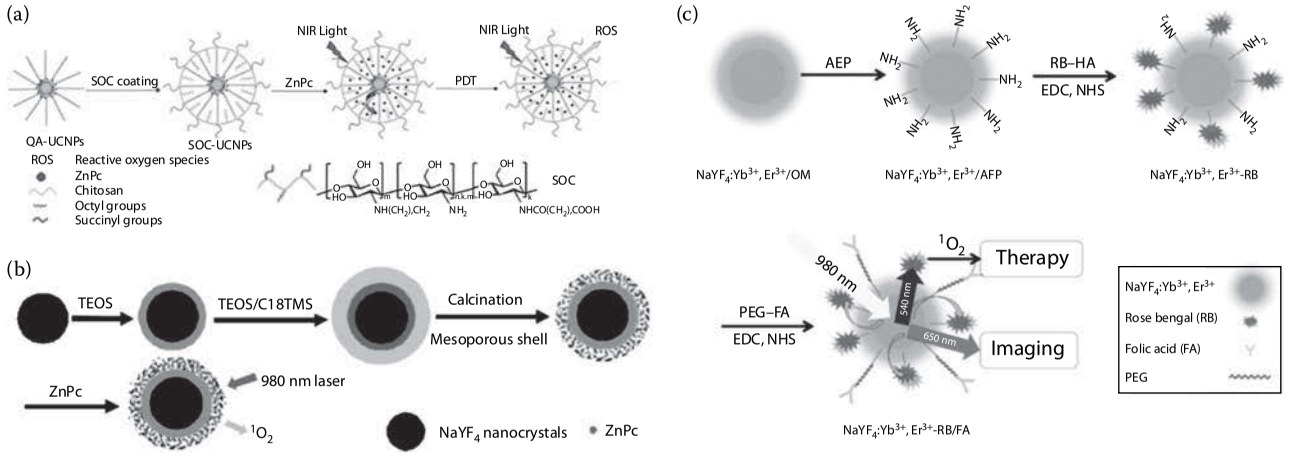

FIGURE 9.2
(a) Schematic showing synthesis of UCNPs encapsulating ZnPc. (b) Schematic showing loading of ZnPc via physical adsorption onto mesoporous silica-coated UCNPs, and (c) UCNPs carrying PS rose bengal attached to the surface covalently. (Reproduced with permission from Cui, S., H. Chen, H. Zhu, J. Tian, X. Chi, Z. Qian, S. Achilefu, and Y. Gu, *J. Mater. Chem.*, 22 (11), 4861–4873, 2012; Qian, H. S., H. C. Guo, P. Chi-Lui Ho, R. Mahendran, and Y. Zhang, *Small*, 5 (20), 2285–2290, 2009; Liu, K., X. Liu, Q. Zeng, Y. Zhang, L. Tu, T. Liu, X. Kong, Y. Wang, F. Cao, and S. A. G. Lambrechts, *ACS Nano*, 6 (5), 4054–4062, 2012, respectively.)

can be encapsulated within amphiphilic micelles. This method has a tunable loading capacity depending on concentration of PS (H. J. Wang et al. 2014), but with the caveat of PS leaking owing to micelle destabilization.

The most common strategy for loading the PS onto the UCNPs is through physical adsorption, primarily because of the ease and simplicity of this approach. Physical adsorption usually involves noncovalent attractive interactions such as hydrophobic interactions or electrostatic forces to attach the PS to the nanoparticle surface. For instance, PSs can be loaded into the pores of mesoporous silica-coated particles through physical adsorption (Figure 9.2b). The pore size of this layer can be adjusted allowing loading of differently sized molecules. In addition, the porous nature of this layer provides a large surface to volume ratio, enabling a greater loading capacity along with better permeability to oxygen and ROS molecules in comparison to silica coating alone (Idris et al. 2012; Qian et al. 2009). Physical adsorption through electrostatic interactions has also been used as a loading strategy. Using this method, a layer-by-layer self-assembly approach can be used, wherein oppositely charged layers can be alternately deposited on the nanoparticle surface, with one of the layers consisting of either the charged PS or a PS conjugated to a charged moiety. With this strategy multiple layers can be deposited, thereby affording a convenient means of controlling the amount of PS loaded. In one such example, a negatively charged Ce6-conjugated polymer was deposited along with a positively charged PAA–poly(allylamine hydrochloride) layer on the UCNP and the process repeated to yield up to three layers of the PS conjugate resulting in a Ce6 loading capacity of 3.4, 7.7, and 11.0 wt% for one-, two-, and three-layered structures, respectively (C. Wang et al. 2013).

The third strategy for loading is through covalent linkage of the PS to the nanoparticle (Figure 9.2c). Here, the PS is usually attached to the UCNP surface through cross-linking agents such as 1-ethyl-3-(3-dimethylaminopropyl)carbodiimide or N,N′-dicyclohexylcarbodiimide. Since the release of the PS from the UCNP surface is not strictly necessary for PDT, this approach provides a viable means of overcoming the problem of premature leakage or release of the PS faced by the other loading strategies mentioned above (Liu et al. 2012; Xu Wang et al. 2014). In fact, covalent linkage has been used for loading PSs onto silica-coated (Zhao et al. 2012) or mesoporous silica-coated UCNPs (Qiao et al. 2012) as well. Furthermore, covalent linkage in conjunction with physical adsorption has also been used to improve loading efficiency (Park et al. 2012). One of the major concerns of this approach is the fact that it requires chemical modification of the PS to enable conjugation, which can potentially reduce the efficacy of the PS. However, most studies have shown that the functional properties of the PS are retained following covalent linkage.

9.2.1.4 In Vitro and In Vivo PDT Using UCNPs

UCNP-based PDT has been demonstrated in cells and in animals, with the first successful proof of concept demonstration by Zhang et al. (2007). This

group used the PS MC540 along with $NaYF_4$: Yb/Er UCNPs and used it to kill MCF-7/AZ breast cancer cells *in vitro*. These cells were incubated with the PS loaded UCNPs and irradiated with NIR light at 974 nm for 36–43 min. In subsequent years, several other groups have also reported UCNP-based PDT in cells with better optimization of PS loading, use of PSs with higher ROS yield, lower UCNP concentrations, and shorter NIR irradiation times at lower power densities. For instance, Chatterjee et al. used ZnPc as a PS and showed 50% cytotoxicity of HT29 human colon cancer cells using 0.733 mg/mL of UCNPs and NIR (980 nm) irradiation time of only 5 min (Chatterjee and Yong 2008). With most of these early reports, the method used for loading the PS onto the UCNPs was either through encapsulation or physical adsorption. In an effort to reduce the leakage of PS as seen with these approaches, covalent linkage to the nanoparticle surface was explored. By reducing PS leakage, a greater amount of the chemical could be delivered to the cells of interest, potentially allowing the use of a lower concentration of PS loaded UCNPs. For instance, Liu et al. (2012) covalently linked the PS rose bengal to the surface of PEG-coated UCNPs. With these particles, 50% of cell death of JAR cells could be achieved using a concentration of only 0.1 mg/mL and NIR (980 nm) irradiation time of 10 min (at 1.5 W/cm^2).

While the initial studies successfully demonstrated the ability of UCNPs as carriers and nanotransducers for PDT, later studies attempted to elucidate the mechanisms behind nanoparticle-mediated PDT. Guo et al. found that cells took up the nanoparticles in a concentration- and time-dependent fashion. When these cells were irradiated with NIR light, the resulting ROS (in this instance singlet oxygen, $^1O_2$) induced oxidative damage caused a change in the nuclear morphology as well as loss mitochondrial membrane integrity evident from the observed chromatin condensation, DNA fragmentation, and release of cytochrome c from the mitochondria. All these events are indicative of apoptosis mediated cell death (Guo et al. 2010).

The efficacy of UCNP-mediated PDT has also been demonstrated *in vivo* in mouse models. The earlier studies usually involved intratumoral injection of PS UCNP-loaded UCNPs. Later, systemic delivery of these particles was also reported with these particles usually modified with targeting moieties in addition to the PS. One of the first studies reporting *in vivo* PDT using UCNPs was by Wang et al. (2011). They used the PS Ce6 and $NaYF_4$:Yb, Er for killing $4T_1$ mouse breast cancer cells and *in vivo* for eradicating a $4T_1$ tumor grown in synergistic mice. The nanoparticles (43 mg/kg) were injected directly into the tumor and the site irradiated with a 980 nm laser for 30 min at 0.5 W/cm^2. This retarded tumor growth, a change not seen in untreated mice. Another report of intratumoral injection was by Cui et al., where they used ZnPc instead of Ce6 (Cui et al. 2012a). They were able to achieve significant retardation of tumor growth at a lower UCNP concentration (33 mg/kg), irradiation power density (0.4 W/cm^2), and NIR irradiation duration (15 min) though irradiation was carried out twice at different time points (30 min in total).

In most cases, the PS is loaded onto the UCNPs using one or more of the three strategies mentioned previously. These strategies have their own advantages and disadvantages with variability in terms of loading efficiency, leakage of PS, etc. In 2015, Zhang et al. reported a different approach to UCNP-based PDT. They uniformly surface coated a photocatalyst titanium dioxide (TiO_2) on a $NaYF_4$:Yb, Tm UCNP core (TiO_2–UCNP) (Lucky et al. 2015). Here, the titania coating itself was the PS. Using this nanoconstruct, cancer cells could effectively be destroyed both *in vitro* and *in vivo*. This approach allowed both a means of controlling the amount of the PS loaded and a way of stably loading it onto UCNPs.

Even though the intratumoral injection studies were beneficial in demonstrating the ability of UCNPs to act as transducers for PDT in solid tumors, their ability as carriers and for tumor specific targeting was brought forth by the subsequent studies reporting systemic injection. When it comes to systemic delivery, there are several other factors that need to be taken into consideration. This route involves the circulation of nanoparticles in the bloodstream before reaching the tumor site. Thus, it becomes necessary to modify the surface with stabilizers such as PEG to improve circulation time, avoid immune detection, etc. In addition, targeting moieties are also used to improve the accumulation of the nanoparticles at the tumor site. Idris et al. (2012) reported intravenous injection of FA–PEG-modified mesoporous silica-coated NaYF:Yb, Er UCNPs, co-loaded with PSs, MC540, and ZnPc (Figure 9.3). They used them for killing B16F0 melanoma in mice and found that that the UCNPs could activate both PSs (through their multiple visible emissions) with a single 980 nm laser excitation. Also, the simultaneous use of two PSs was more effective in reducing tumor volume than using a single one. A UCNP dose of 50 mg/kg and a long-exposure time of 60–120 min of the 980 nm light at 0.415 W/cm^2 was required for effective PDT treatment. Park et al. (2012) reported another systemic delivery system. They used a much lower UCNP dose of 5 mg/kg of the UCNP with only 5 min of exposure to 0.6 W/cm^2 of 980 nm light for effective inhibition of the U87-MG human glioblastoma tumor growth. Here, they used Ce6 as the PS, which was loaded onto the UCNPs through both physical adsorption and covalent linkage. This dual loading strategy resulted in high loading efficiency, thereby effectively lowering the dosage of PS loaded UCNPs needed for PDT.

9.2.2 Photochemical Internalization

A major challenge in the delivery of biomolecules is the poor efficiency of cytoplasmic delivery (due to poor endosomal escape) especially when using nanoparticles, since cells clear away the foreign nanoparticles, reducing the effective concentration of nanoparticles accumulated inside the cells. In addition, lysosomes are highly acidic (pH ~4.5) and contain nucleases that can degrade payload such as nucleic acids. Thus, poor endosomal release

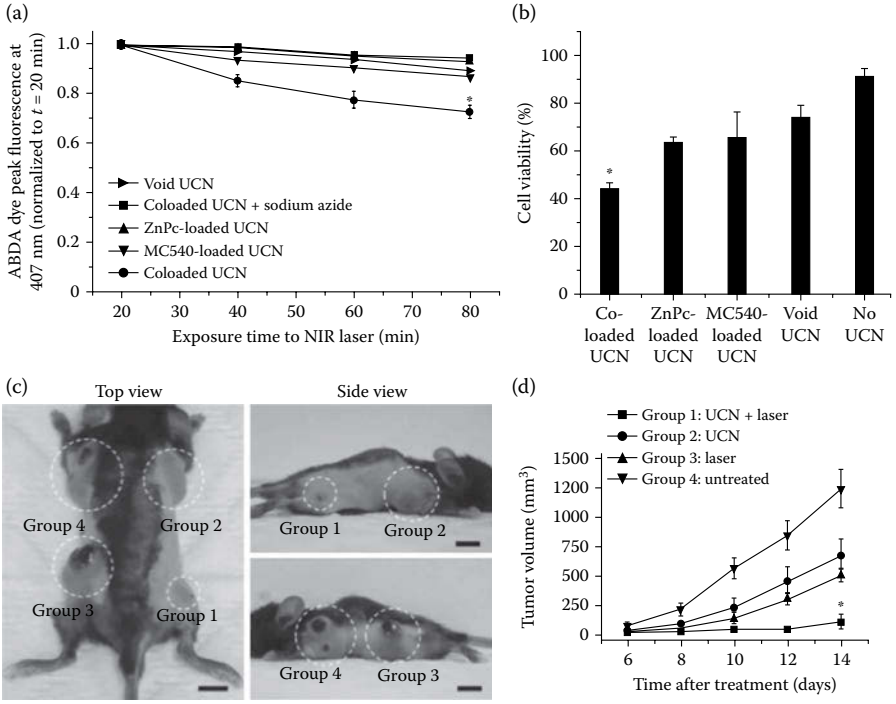

FIGURE 9.3

(a) Comparison of singlet oxygen production between coloaded, MC540-loaded, ZnPc-loaded, and void UCNPs under 980-nm NIR irradiation (2.5 W/cm^2) as determined by the decay of 9,10-anthracenediyl-bis(methylene)dimalonic acid (ABDA) fluorescence. (b) 3-(4,5-dimethylthiazol-2-yl)-5-(3-carboxymethoxyphenyl)-2-(4-sulfophenyl)-2H-tetrazolium assay for measuring cell viability to test efficacy of PDT treatment (by exposing cells that have taken up differentially loaded UCNPs to 2.5 W/cm^2 of 980-nm NIR laser for 40 min). (c) Representative gross photos of a mouse showing tumors (highlighted by dashed white circles) at 14 d after treatment with the conditions described for groups 1–4. Scale bars, 10 mm. (d) Tumor volumes in the four treatment groups at 6, 8, 10, 12, and 14 days after treatment to determine the effectiveness of the treatment in terms of tumor cell growth inhibition. Values are means ± scanning electron microscopy (SEM) (n = 6 mice per group). (Reproduced with permission from Idris, N. M., M. K. Gnanasammandhan, J. Zhang, P. C. Ho, R. Mahendran, and Y. Zhang, *Nat. Med.*, 18 (10), 1580–1585, 2012. http://www.nature.com/nm/journal/v18/n10/abs/nm.2933.html#supplementary-information.)

combined with harmful conditions in the late endosomes and lysosomes constitute a major hurdle in therapy (Berg et al. 2006). Various strategies have been used to overcome this issue and one such effective solution utilizing light is PCI.

This technology employs specific, preferably amphiphilic, photosensitizing compounds, which accumulate in the membranes of the endocytic vesicles. When the cells are illuminated with light of a specific wavelength, these photo sensitizers (PS) become excited and subsequently induce the formation of ROS, primarily singlet oxygen. The short range of action and

short lifetime confines the damaging effect of these ROS to the production site (Oliveira et al. 2007). This localized effect induces the disruption of the endocytic vesicles, thereby releasing the entrapped therapeutic molecules into the cytosol before they are transferred to the lysosomes (Dominska and Dykxhoorn 2010). This technique thus provides an added dimension of spatial and temporal control over biomolecule delivery, making therapy more specific and effective.

9.2.2.1 Photosensitive Chemicals for PCI

Several different PSs have been reported for PCI with most of them based on porphyrin structures. The most popular of these is tetraphenylporphine disulfonate (TPPS2a) developed by Hogset et al. (PCI Biotech), and has been reported by several groups to improve therapeutic efficacy of drug and gene delivery systems incorporating this chemical (Boe et al. 2010; Fretz et al. 2007; Oliveira et al. 2007; Selbo et al. 2006). Recently, another PS TCPS2a (Berstad et al. 2012), developed by the same group is gaining prominence with several advantages over TPPS2a such as improved amphiphilicity and red shifted absorption (Lilletvedt et al. 2011). Some of the other PSs used in PCI include aluminum disulfonate phthalocyanine (AlPcS2a) (Jin et al. 2011), rhodamine (Gillmeister et al. 2011), etc. These PSs produce ROS similar to those used in PDT. However, these PSs accumulate preferentially in the endocytic vesicles, are used in minute concentrations producing ROS that is sufficient to rupture the endosomes but not kill the cell.

Initial demonstrations of PCI were done *in vitro* wherein cells were co-incubated with the PS and the molecule to be delivered. After about 18 h of incubation, the cells were irradiated with UV or visible light (depending on the PS used). These studies revealed that efficacy of biomolecule delivery into the cytoplasm and thus, the resulting therapeutic efficacy were higher with PCI. An *in vivo* demonstration of PCI in improving gene transfection efficiency was done by Nishiyama et al. They used a ternary complex composed of a core comprising of DNA packaged with cationic peptides which was enclosed in the anionic dendrimer phtalocyanine. Phtalocyanine acted as a PS in this study. With PCI, the gene transfection was enhanced 100 fold. The animal experiments were done in rats where the complexes were introduced via subconjuctival injection (in the eye) (Nishiyama et al. 2005). Although these studies demonstrated the utility of PCI in enhancing cytoplasmic delivery of biomolecules, the fact that the photosensitizers were sensitive to UV/visible light limited their *in vivo* potential.

In 2014, Jayakumar et al. synthesized novel NIR-to-UV/vis UCNPs made up of a ore–shell architecture, which upon NIR excitation emit across the UV and visible range. These emissions were used to excite multiple photoactive molecules simultaneously, namely PS (TPPS2a) for PCI (visible emission) and photoresponsive nucleic acid (anti-STAT3 photomorpholino) for gene knockdown

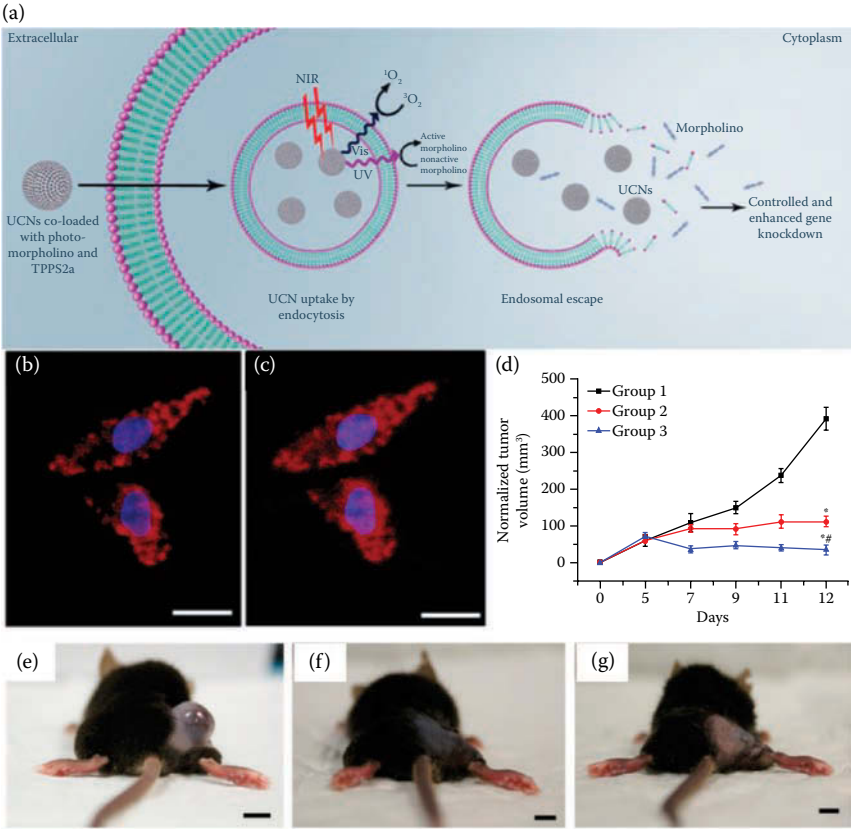

FIGURE 9.4
(a) Schematic showing simultaneous endosomal escape (PCI) and uncaging of nucleic acid using UCNPs. Distribution of UCNPs before (b) and after (c) NIR irradiation (scale bar: 5 µm): UCNPs, red; 2-(4-amidinophenyl)-1H-indole-6-carboxamidine (DAPI), blue. A more diffuse pattern shows cytosolic release after endosomal escape. (d) Change in tumor volume as a function of time to assess the effectiveness of simultaneous activation of TPPS2a (for PCI) and STAT3 photomorpholino for treating B16F0 melanoma tumor in C57 Bl/6 mice. Values are means ± SEM (n = 6 mice per group). Group 1, saline control; group 2, UCNPs loaded with photomorpholinos and irradiated with NIR laser; and group 3, UCNPs co-loaded with photomorpholinos and TPPS2a and irradiated with NIR laser. Representative gross photos of a mouse from each group 1–3 (e–g). Scale bar: 1 cm. (Reproduced with permission from Jayakumar, M. K. G., A. Bansal, K. Huang, R. Yao, B. N. Li, and Y. Zhang, *ACS Nano*, 2014.)

(UV emission) (Figure 9.4). These nanoparticles were coated with mesoporous silica and co-loaded with both the PS and nucleic acid. They were then added to B16F0 mouse melanoma cells *in vitro* or injected intratumorally into a B16F0 melanoma tumor grown in C57bl/6 mice. With PCI, the endosomal release of the anti-STAT3 photomorpholino was enhanced both *in vitro* and *in vivo*. This resulted in improved gene knockdown and thus reduction in tumor volume that was several folds higher (Jayakumar et al. 2014).

9.3 Photocontrolled Release of Molecules

Photocontrolled release of biomolecules can be achieved in several ways. The molecule itself can be modified using a photolabile group that renders it "inactive," in a process called photocaging or it can be attached to the surface of a carrier via a photolinker. Alternately, it can also be encapsulated within a carrier composed of photosensitive group modified components. In either case, upon irradiation with light of a suitable wavelength, the photolabile group cleaves resulting in either "activation" of the molecule, release of the biomolecule from the surface of the carrier, or dissociation of the carrier and subsequent release of cargo contained within, respectively. Photocaging is a popular technique for using light to achieve site-specific activation of biomolecules. It involves modifying the molecule to be delivered (plasmid/siRNA/drug, etc.) using a photolabile moiety. This renders the molecule nonfunctional (Sortino 2012). When the desired delivery site is irradiated with light of a suitable wavelength (usually UV light), this photolabile group gets released, thereby rendering the molecule functional or active again. This process of covalently linking the photolabile group to a biomolecule is termed "caging" and the biomolecule is said to be "caged" (Yu et al. 2010). In most biomolecules, certain key functional groups are responsible for bioactivity. Photocaging works by blocking these key functional groups (carboxyl groups, amino groups, phosphate moieties, hydroxyl groups, etc.) using photolabile molecules, thereby, hindering their bioactivity.

The process of photocaging allows us to achieve site-specific activation of biomolecules via irradiation of the region of interest. Besides caging biomolecules directly, photolabile groups that act as linkers have also been used for controlled release. This involves attaching the desired molecule to a carrier via a linker that can be cleaved upon irradiation with light of a suitable wavelength to which it is sensitive (Yang et al. 2013a). Although the manner in which the release of the desired molecule is achieved is different for this technique in comparison to photocaging, the basic premise of using a photolabile group remains the same with a similar end result. This section will describe some of the commonly used photolabile groups used in photocontrolled delivery systems, UCNP-based strategies for photocontrolled delivery, and application in cells and in animals.

9.3.1 Photolabile Groups in Photocontrolled Delivery

There are certain criteria that photolabile groups used in photocontrolled delivery systems intended for biological use need to meet. These include high quantum yield of the photoreaction, high absorption coefficient of the group, safe photochemical by-products, and solubility in aqueous solvents (Pelliccioli and Wirz 2002). Several different types of photolabile molecules have been developed for this purpose and can be divided into

several categories depending on the mechanism of photolysis. These include: o-nitrobenzyl (NB) and related groups (e.g., nitrophenyl ethyl (NPE), o-NB, 1-(4,5-dimethoxy-2-nitrophenyl) diazoethane (DMNPE)), coumarin-4-ylmethyl and related groups (e.g., 7-methoxycoumarin-4-ylmethyl), p-hydroxyphenacyl (pHP) group (a promising alternative to the NB-based groups to cage biomolecules), and other miscellaneous groups such as nitroindolinyl (NI), 4-methoxyl-7-nitroindolinyl, and benzoin (Pelliccioli and Wirz 2002; Yu et al. 2010) (Figure 9.5). These groups are modified through the addition of certain substitution groups in the basic framework of the photolabile

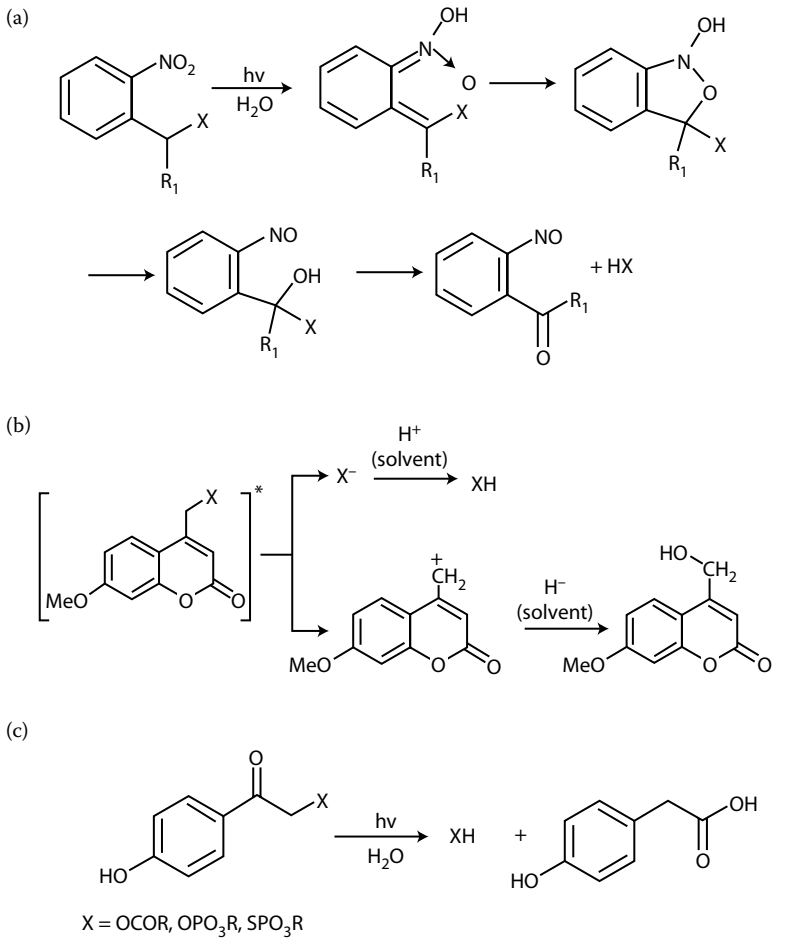

FIGURE 9.5
Mechanism of photolysis of (a) NB (R_1 = H) or NPE (R_1 = Me) caged compounds, (b) coumarin-4-ylmethyl caged compounds, and (c) pHP caged carboxylates, phosphates, and thiolphosphates. (Reproduced with permission from Yu, H., J. Li, D. Wu, Z. Qiu, and Y. Zhang, *Chem. Soc. Rev.*, 39 (2), 464–473, 2010. doi: 10.1039/b901255a.)

molecule to attain the aforementioned properties desirable for biological use such as good aqueous solubility, long-wavelength absorption (redshift), and high absorption coefficient (Yu et al. 2010).

o-NB derivatives are the most common photolabile protecting groups. This group is synthetically incorporated into the molecule to be caged via linkage to a heteroatom (usually *O*, *S*, or *N*) as an ether, thioether, ester, amine, or similar functional group. Although very effective, NB cages have some distinct disadvantages. These include toxic by-products and slow release rates following excitation.

A promising alternative to o-NB derivatives is the pHP group. pHP is used to cage mostly carboxylates and phosphates and has a fast release rate following excitation. In addition, aqueous solubility, nontoxic by-products, high stability under physiological conditions, makes this group very attractive. However, a disadvantage is the relatively low absorption coefficient at wavelengths above 320 nm.

A relatively new player in this field is the Coumarin-4-ylmethyl group and its derivatives. It can be used to cage carboxylic acids, phosphates, amino group as well as the hydroxyl group. It has a high absorption coefficient and fast release rate making it suitable for a host of applications (Yu et al. 2010).

9.3.2 UCNP-Based Phototriggered Release *In Vitro* and *In Vivo*

Most of the photolabile groups described in the previous section respond to UV light. Not only is UV light toxic, it also has low tissue penetration, which makes it unsuitable for use in a clinical setting. Thus, the use of UCNPs as NIR to UV transducers is advantageous particularly for *in vivo* delivery and site-specific activation of bioactive molecules such as drugs, nucleic acids, etc. There are several strategies for employing UCNPs in photocontrolled delivery systems. They can be deployed as transducers for and carriers of photocaged biomolecules. When the region of interest is irradiated with NIR light, the upconverted light from the UCNPs uncages the biomolecules, rendering them functional. UCNPs can also be co-encapsulated with caged biomolecules within a larger particle (with a porous surface) in a "yolk–shell" approach, such that irradiation with NIR light uncages the biomolecule which then diffuses out of the pores of the larger particle in its active from. Lastly, UCNPs have also been co-encapsulated with the cargo to be delivered in hydrogels and micelles made of components that contain photolabile groups. Upon irradiation with NIR light, the photolabile group is cleaved due to the upconverted light produced by the UCNPs, resulting in disruption of the hydrogel or micelle and releasing the contents confined within.

One of the earliest reports of using UCNPs for NIR triggered uncaging was by Carling et al. (2010). They used a benzoin cage to modify a model molecule, which upon uncaging released carboxylic acid. Although not of therapeutic use, this study showed that UCNPs could be used as transducers for NIR-based uncaging of molecules. This generated a lot of interest in this

field with subsequent reports of NIR mediated uncaging of small molecules and bioactive moieties for therapeutic use. For instance, Garcia and group reported photoactivation of caged nitric oxide with potential applications in cancer treatment (Garcia et al. 2012). Caged chemotherapeutic drugs can also be uncaged in a site-specific manner using UCNPs upon irradiation with NIR light. Dai et al. used $NaYF_4$: Yb/Tm @ $NaGdF_4$ UCNPs for photocontrolled delivery of the light-activated prodrug dipeptidyl-peptidase (DPP) (trans,trans,trans-[$Pt(N_3)_2$-$(NH_3)(py)(O_2CCH_2CH_2–COOH)_2$]) and multimodal imaging (Dai et al. 2013). The upconverted UV light from the UCNPs activated the prodrug to its active form. They used these prodrugs loaded particles *in vitro* in HeLa cells. Significant reduction in cell viability was seen when cells were incubated with drug-loaded UCNPs and irradiated with NIR. Irradiation with NIR light alone did not cause such a toxic effect. These prodrug loaded particles were also tested *in vivo* in a mouse model with H22 xenografts. NIR irradiation upon treatment with these prodrug-loaded particles caused excellent inhibition of tumor growth. In addition, the Gd doping allowed these particles to be used for MRI and the presence of Yb and Gd ions for computed tomography imaging. Thus, this platform allowed for both targeted delivery of a chemotherapeutic drug and multimodal imaging. Zhao et al. demonstrated an interesting approach for using UCNPs for photocontrolled drug delivery. They synthesized yolk–shell particles, each consisting of a single UCNP yolk and mesoporous silica shell. The coumarin-caged chemotherapeutic drug chlorambucil was adsorbed in the space between the UCNP yolk and mesoporous silica shell. Upon irradiation with NIR light, the upconverted UV light produced by the UCNPs uncaged the drug, which diffused out of the pores of the shell in its active form. This system was tested both *in vitro* and *in vivo* (Zhao et al. 2013) (Figure 9.6a–g). Instead of modifying the drug directly, photocontrolled delivery using mesoporous silica-coated UCNP can also be achieved by loading the drug of interest into the pores and then covering or "capping" the pore with a photolabile group (J. Liu et al. 2013; Yang et al. 2013b). Upon irradiation with NIR light, the upconverted light from the UCNPs cleaves the capping group, leaving the cargo free to diffuse out of the pores. Besides drugs and small molecules, UCNPs have also been used for photocontrolled delivery of nucleic acids such as plasmids, siRNA, photomorpholinos, etc. Jayakumar et al. demonstrated the use of NIR to UV UCNPs in achieving spatially and temporally controlled gene expression/knockdown with the use of caged siRNA and plasmid (Jayakumar et al. 2012). Green fluorescent protein (GFP) plasmid was caged using DMNPE [1-(4,5-DMNPE] and loaded onto mesoporous silica-coated UCNPs. When cells were incubated with these particles and irradiated with NIR light, strong GFP expression was observed which was absent in cells not irradiated with NIR light (Figure 9.6h–j). GFP expression in cells expressing this protein could also be knocked down using caged anti-GFP plasmid upon irradiation with NIR light. In addition, the toxicity of the mesoporous silica-coated UCNPs was minimal at the concentration

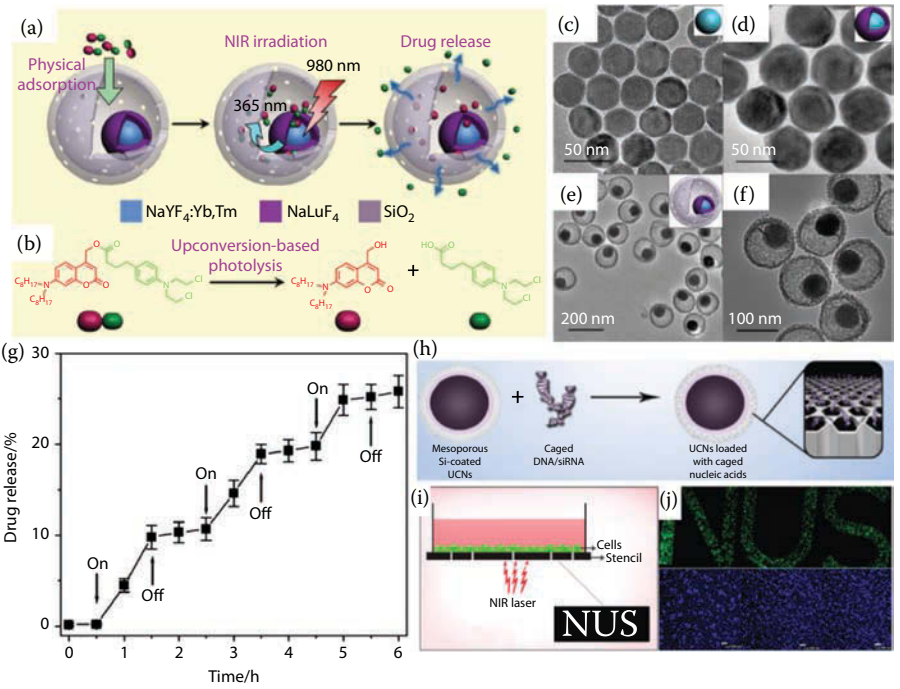

FIGURE 9.6
(a) Schematic illustration of the NIR-regulated upconversion-based drug delivery and (b) the photolysis of the prodrug under upconversion emission from the yolk–shell UCNPs (YSUCNPs). Transmission electron microscopy (TEM) images of the (c) NaYF:Yb,Tm, (d) NaYF:Yb,Tm@ NaLuF, and (e, f) YSUCNP nanoparticles. (g) The photoregulated release of chlorambucil (drug) from YSUCNP-ACCh controlled by a 980 nm laser. "ON" and "OFF" indicate the initiation and termination of laser irradiation, respectively. The working power density of the 980 nm laser was 570 mW/cm^2. (h) Schematic showing loading of caged plasmid DNA/siRNA into the mesopores of UCNPs. (i) Schematic of setup showing the stencil and the position of the laser for patterning of cells transfected with caged pGFP. Inset shows the pattern (National University of Singapore [NUS]) on the stencil. (j) Composite image showing the GFP fluorescence from three different wells (one letter in each well of a 96-well plate) (scale bar, 200 µm) and live-cell DAPI staining of the same to show the cell confluence. (Reproduced with permission from Zhao, L., J. Peng, Q. Huang, C. Li, M. Chen, Y. Sun, Q. Lin, L. Zhu, and F. Li, *Adv. Funct. Mater.*, 2013. doi: 10.1002/adfm.201302133; Jayakumar, M. K., N. M. Idris, and Y. Zhang, *Proc. Natl. Acad. Sci. USA*, 109 (22), 8483–8488, 2012. doi: 10.1073/pnas.1114551109, respectively.)

used in the experiments (0.5 mg/mL). Thus, this method was able to achieve very efficient photo uncaging of nucleic acids using deep penetrating and nontoxic NIR light, thereby overcoming the limitations associated with traditional methods for photocontrolled gene delivery. Yang et al. also used NIR to UV UCNPs to demonstrate photocontrolled gene expression/knockdown. However, instead of loading photocaged nucleic acids, they functionalized the surface of their silica-coated UCNPs with a photoresponsive o-NB linker terminating with a positively charged alkyl amine group and used

electrostatic interactions with negatively charged siRNA to achieve loading. Upon irradiation with NIR, the photolinker was cleaved resulting in siRNA release. This system was demonstrated *in vitro* by knocking down GFP using a Si-UCNP-photolinker-anti-Enhanced green fluorescent protein (EGFP) siRNA complex upon irradiation at 980 nm (Yang et al. 2013a).

In 2014, Jayakumar et al. also showed simultaneous photoactivation of two different molecules. They synthesized core–shell $NaYF_4$: Yb, Tm@$NaYF_4$: Yb, Er UCNPs that could emit across the UV and visible range upon irradiation with NIR light at 980 nm. These particles were coated with mesoporous silica and co-loaded with photomorpholino (anti-STAT3) and TPPS2a, a PS used for PCI. B16F0 murine melanoma cells (overexpressing STAT3) were incubated with these particles and irradiated with NIR light. The visible emission of the UCNPs activated TPPS2a resulting in improved endosomal escape (and release of cargo into the cytoplasm) and the UV emission activated the photomorphoino. This resulted a significant reduction in STAT3 levels and cell death as compared to delivery of photomorpholino alone. Similar results were seen *in vivo* in a mouse melanoma model.

UCNPs have also been used for disrupting photosensitive hydrogels and micelles containing the molecules to be delivered encapsulated within. Yan et al. (2011) synthesized micelles using block copolymers [poly(ethylene oxide)-block-poly(4,5-dimethoxy-2-NB methacrylate)] and encapsulated NaYF:Yb, Tm UCNP in them. Upon irradiation with an NIR laser, the UCNPs produced UV light which caused the photocleavage of o-NB groups in the micelle, micelle dissociation, and release of a dye molecule contained within. Although this study used a dye molecule to demonstrate the concept, this system can be applied for delivery of therapeutic cargo. The same group also used UCNPs ($NaYF_4$: Yb/Tm) to achieve temporally controlled release of biomolecules entrapped in a hydrogel (Yan et al. 2012). They prepared a hydrogel, with a cross-linked hybrid polyacrylamide–PEG structure held together by photoresponsive o-NB groups. The UCNPs and desired biomolecules were entrapped in this hydrogel. Upon irradiation with NIR at 980 nm, the UCNPs emitted UV light, which resulted in the cleavage of the UV sensitive o-NB groups, releasing the entrapped biomolecules in the process. The release of the biomolecules was dependent on the laser power, allowing for a stepwise (not continuous) release. It is important to note that these experiments made use of very high laser power (3–5 W) and for prolonged time periods (30 min and above). This is a potential limiting factor for the use of this method *in vivo*.

9.4 Photothermal Therapy

PDT though promising, has certain limitations in that it is dependent on the oxygen levels in the tumor. Consequently, it is potentially less effective

in hypoxic conditions where the oxygen partial pressure can fall below 40 mmHg (common in large tumors) (Henderson and Fingar 1987; Mitchell et al. 1985; See et al. 1984). Thus, a therapy that is independent of oxygen levels is beneficial in this regard. PTT is one such modality. It is similar to PDT in that it uses a medium, which upon irradiation with light of a suitable wavelength results in cell death, with the major difference being the mechanism of cell kill. In case of PDT, the PS upon irradiation produces ROS but in PTT, the light absorbed is converted to heat. This raises the temperature of the local environment to more than 41°C (hyperthermia) and causes irreversible cell damage (Boulnois 1986; Nikfarjam et al. 2005)

The nonspecific damage to the surrounding healthy tissue had made it impractical to use hyperthermia as a mode of cancer therapy earlier but PTT has allowed researchers to use a noninvasive stimulus such as light to induce hyperthermia in a controlled and localized manner, thereby making it a viable and effective option that can be used to treat tumors even under hypoxic conditions (Boulnois 1986; C. Jin et al. 2013; Nikfarjam et al. 2005).

The key consideration for a PS or any light to heat transducer suitable for this technique is the efficacy of this conversion. Although naphthalocyanines and metal porphyrins have been used frequently, they are prone to photobleaching under laser irradiation, which greatly reduces their therapeutic potential (Camerin et al. 2005). Recently, gold nanoparticles have become increasingly popular as they offer excellent light to heat conversion due to the surface plasmon resonance (SPR) oscillation, high absorption cross section of NIR light, and good photostability. Thus, they can be used to achieve PTT in deeper tissues and for a prolonged duration of time (Hu et al. 2006; Huang et al. 2008; Nakamura et al. 2010; O'Connell et al. 2002). Other plasmonic metals like silver have also been used for the same.

9.4.1 UCNP-Based PTT

Besides the use of gold and silver nanoparticles, UCNPs coated with these materials have also been used for PTT. Use of UCNPs provides the added advantage of simultaneous imaging owing to their multiple visible and/or NIR emissions. Dong et al. demonstrated the use of silver-coated UCNPs for image guided PTT. They synthesized UCNPs with a $NaYF_4$ core doped with ytterbium, that is, Yb^{3+} (absorber/donor ion) and erbium, Er^{3+} (emitter/acceptor ion). These UCNPs are excited at NIR 980 nm and emit in the visible range (green and red regions). They were then coated with silver (Ag), resulting in a core–shell structure with a UCNP core and Ag shell. Ag, a plasmonic metal was chosen owing to its good photothermal properties and the thickness of the shell was tuned so that the SPR absorption was at 980 nm. These particles could be used for imaging (due to the visible emissions of the UCNPs) and PTT (due to the SPR of the Ag shell) simultaneously upon excitation with NIR at 980 nm. These particles were tested out *in vitro* but not *in vivo*. The toxicity of these particles, though lower than that of the UCNP core

alone, was significant and increased with increasing particle concentration. In fact, the concentration used for *in vitro* therapy (1 mg/mL) caused about 50% cell death even without NIR irradiation, a serious drawback that might limit their *in vivo* potential (Dong et al. 2011).

UCNPs coated with gold have also been used for PTT. Qian et al. (2011) synthesized $NaYF_4$:Yb, Er/$NaYF_4$/silica (core/shell/shell) UCNPs (~70–80 nm) and deposited gold nanoparticles (~6 nm) on the surface of the silica shell of these nanoparticles. The UCNPs were excited by NIR and the upconverted green light was coupled with the surface plasmon of Au leading to rapid heat conversion, resulting in the destruction of BE (2)-C (neuroblastoma) cancer cells. Cheng et al. prepared multifunctional particles in which UCNPs were coated in a layer-by-layer manner first with iron oxide nanoparticles and then with a gold shell, followed by PEG coating to impart aqueous stability. The gold coating was utilized for NIR-mediated PTT while the UCNP luminescence and iron oxide allowed for dual-modal luminescence and MRI (Cheng et al. 2011). These particles were used for killing cancer cells *in vitro* and their potential for tumor imaging was analyzed *in vivo.* PTT *in vivo* was not demonstrated. The same group later demonstrated the use of these particles for *in vivo* PTT and multimodal imaging. In this study, the multifunctional UCNPs were intravenously injected and then magnetically targeted to the tumor site though the application of an external magnetic field, followed by irradiation of the tumor site with NIR light (Figure 9.7). This approach resulted in 8-fold higher tumor uptake of UCNPs and subsequently an enhanced tumor ablation effect (Cheng et al. 2012).

9.5 UCNPs in Combination Therapy

UCNPs can have multiple emission peaks and can be modified to carry multiple molecules simultaneously. This has led to an advent of UCNP-based combination therapies, wherein these particles are used as carriers and/or transducers for delivery and activation of multiple photoresponsive molecules for a synergistic therapeutic effect. For instance, there have been reports of UCNP-based therapies combining PDT and PTT, PDT and drug/gene delivery, as well as trimodal PDT, chemo- and radiotherapy. Y. Wang et al. (2013) used UCNPs covalently grafted with nanographene oxide (NGO) via bifunctional PEG for combined PDT and PTT along with tumor imaging . The NGO coating has a strong absorption coefficient in the NIR range and can be used for PTT. Next, the PS ZnPc was loaded onto the NGO coating. Upon irradiation with light at 808 nm, the NGO coating caused a localized heating effect resulting in cancer cell kill through PTT. Irradiation with 630 nm light-activated ZnPc and caused cell kill via PDT. Irradiating HeLa cells incubated with these nanocomposites with both 808 and 630 nm light

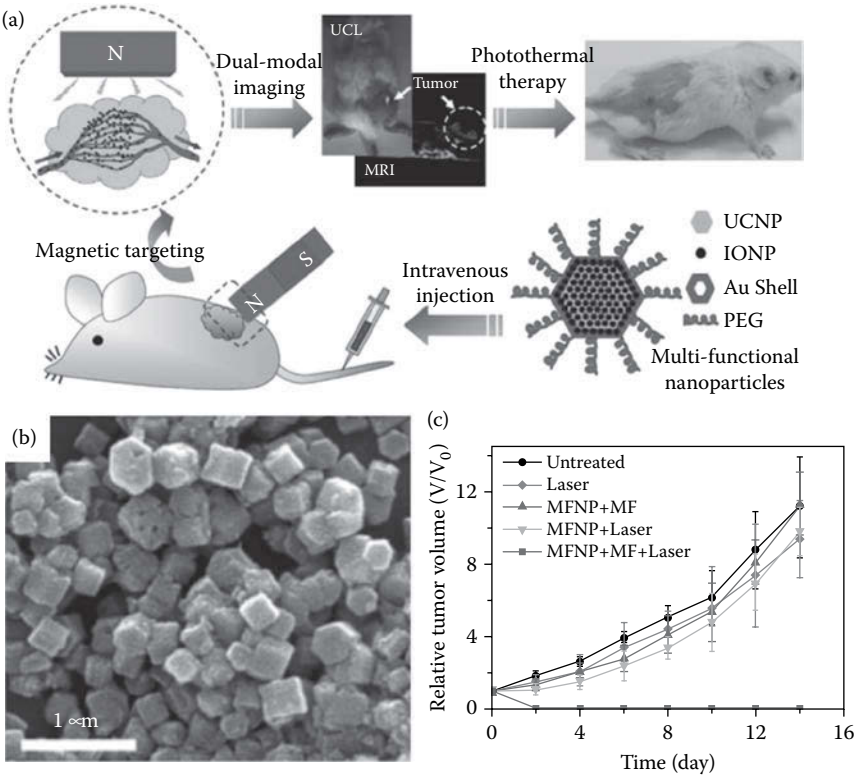

FIGURE 9.7
(a) Schematic illustration showing the composition of multifunctional nanoparticles (MFNP) and the concept of *in vivo* imaging-guided magnetically targeted PTT. The magnetic field around the tumor region induces local tumor accumulation of MFNPs. (b) An SEM image of MFNP-PEG. (c) Treatment of tumor *in vivo* using UCNP-mediated PTT. The growth of $4T_1$ tumors in different groups of mice after treatment. The tumor volumes were normalized to their initial sizes. For the treatment group, eight mice injected with MFNP-PEG were placed under the tumor-targeted magnetic field for 2 h and then exposed to an 808-nm laser at a power density of 1 W/cm^2 for 5 min. Other four groups of mice (seven mice per group) were used as controls: (1) no MFNP injection and no laser (untreated); (2) laser only without MFNP injection (laser); (3) injected with MFNP under the magnetic field but without no laser irradiation (MFNP + MF); and (4) injected with MFNP and exposed to the laser but without the magnetic targeting. Error bars were based on standard deviation (SD). (Reproduced with permission from Cheng, L., K. Yang, Y. Li, X. Zeng, M. Shao, S.-T. Lee, and Z. Liu, *Biomaterials*, 33 (7), 2215–2222, 2012.)

resulted in a synergistic cell kill effect, which was greater than that seen with either of the therapies individually. Interestingly, this study did not use the upconversion property of UCNPs for PTT or PDT; rather UCNPs were used as carriers and their upconverted light used for imaging alone.

Yuan and group reported combined chemotherapy and PDT triggered via upconverted light produced by UCNPs (Yuan et al. 2014). They covalently attached a chemotherapeutic drug doxorubicin (DOX) to a PEGylated

conjugated polyelectrolyte (CPE) PS through a UV-cleavable o-NB linker. This CPE–DOX was used to encapsulate hydrophobic UCNPs in aqueous media. When irradiated with NIR light, the UV linker cleaved due to the upconverted UV light produced by the UCNPs. In addition, the upconverted visible light activated the photosensitzer, resulting in ROS production. Thus, by utilizing the multiple emission peaks of UCNPs, both photocontrolled delivery of a chemotherapeutic drug and PDT could be achieved. This system was demonstrated *in vitro* using U87-MG glioblastoma cells. A similar approach was used by Xin Wang et al (2014) for combined PDT and gene therapy.

A trimodal synergistic therapy using UCNPs was demonstrated by Fan et al. (2014). They synthesized Gd-doped UCNPs with a mesoporous silica core, with a cavity between the core and the shell. Hematoporphyrin (a PS that doubles up as a radiosensitizer) was encapsulated in the space between the UCNP core and mesoporous silica shell. A radiosensitizer/chemodrug docetaxel (Dtxl) was covalently grafted onto the shell. This nanocomposite was used for theranostics, that is, both diagnostics and therapy. Gd doping allowed for MRI, which in combination with upconversion luminescence was used for locating the tumor. NIR excitation and X-ray irradiation resulted in combined radio–chemo therapy and PDT. This nanotheranostic platform was tested both *in vitro* using HeLa cells and *in vivo* in $4T_1$ tumor bearing mice. Maximum reduction in tumor volume was seen in mice exposed to both NIR light and X-ray radiation (trimodal therapy) and was significantly higher than that observed for individual modalities (Figure 9.8).

9.6 Limitations of UCNPs

UCNPs have provided a simple yet effective means of using NIR light for photoactivation applications that had long relied on UV or visible light. Although this has brought these techniques closer to clinical use, UCNPs are not without their limitations. The quantum yield of these particles is very low, usually less than 1% (Cheng et al. 2013). As a result, a relatively high intensity of NIR is required to obtain emission levels sufficient for photoactivation and imaging. In addition, most UCNPs are excited by NIR at 980 nm, a wavelength close to the absorption peak of water molecules. This combined with the high laser power required for excitation can result in significant tissue heating. These problems pose a barrier to the widespread use of UCNPs in therapy. As a result, tremendous efforts are being made toward improving quantum yield and developing UCNPs with alternate excitation wavelengths.

Quantum yield of UCNPs has been improved through optimization of dopant ratios and dopant types use of different host materials and through coating with an undoped shell such as $NaYF_4$ or CaF_2. The addition of an undoped layer around the particles reduces nonradiative excitation losses

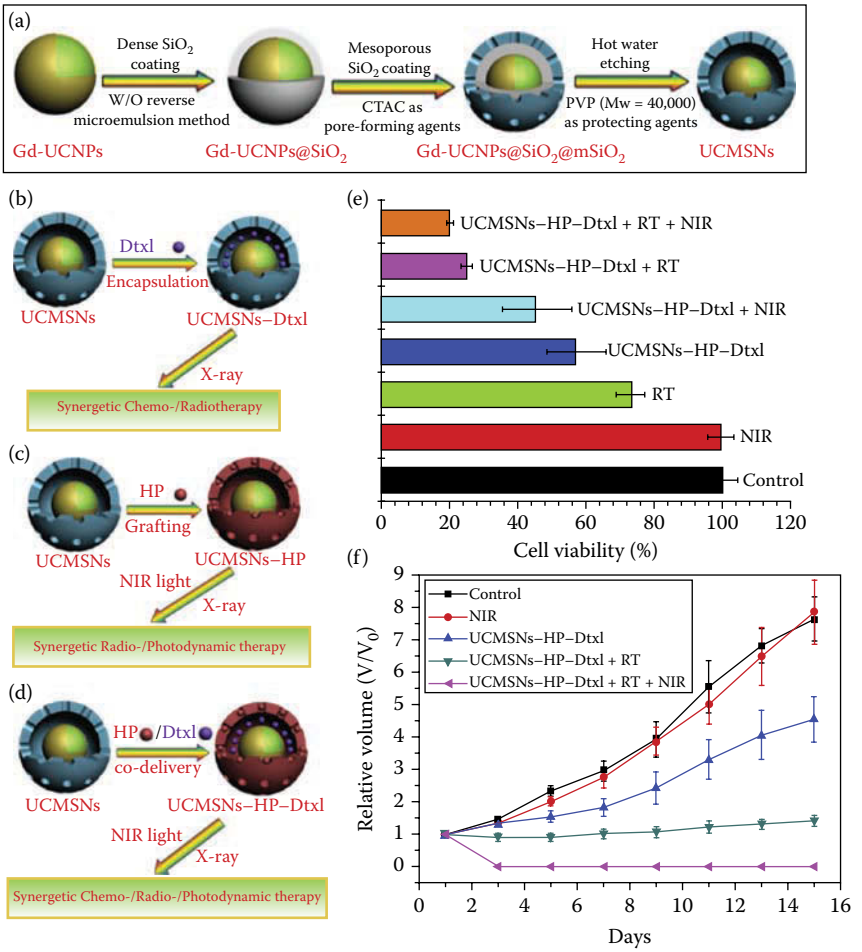

FIGURE 9.8

(a) Schematic illustration of the synthetic procedure of UCNPs core/mesoporous silica shell nanotheranostics (UCMSNs). Gd-UCNPs were prepared by epitaxial growth $NaGdF_4$ layer on $NaYF_4$:Yb/Er/Tm through a typical thermal decomposition process. Then, a dense silica layer was coated on Gd-UCNPs by a reverse microemulsion method producing Gd-UCNPs@SiO_2. Subsequently, a mesoporous silica shell was deposited on Gd-UCNPs@SiO_2 via the template of cetyltrimethylammonium chloride (CTAC) resulting in Gd-UCNPs@SiO_2@$mSiO_2$. Finally, UCMSNs were successfully fabricated based on a "surface-protected hot water etching" strategy. (b) Schematic diagram of synergetic chemo-/radiotherapy effects of free Dtxl/UCMSNs-Dtxl, (c) Synergetic radio-/PDT effects of UCMSNs–HP and (d) schematic diagram, and (e) *In vitro* evaluation of synergetic chemo-/radio-/PDT effects on HeLa cells after co-incubated with 5 mg/mL UCMSNs-HP-Dtxl. (f) *In vivo* evaluation of synergetic chemo-/radio-/PDT on $4T_1$ tumor bearing mice after intravenous injection of UCMSNs–HP–Dtxl. Tumor growth curves of $4T_1$ tumor bearing mice over a period of half a month after the corresponding treatments. Control groups received phosphate buffered saline (PBS). (Reproduced with permission from Fan, W., B. Shen, W. Bu, F. Chen, Q. He, K. Zhao, S. Zhang, L. Zhou, W. Peng, and Q. Xiao, *Biomaterials*, 35 (32), 8992–9002, 2014.)

at the particle surface thereby improving upconversion emission (Heer et al. 2004). Development of UCNPs with alternative excitation wavelengths different from the conventional 980 nm has been achieved through the use of novel dopants like neodymium (Nd^{3+}) and different lattice structures. UCNPs doped with neodymium ions (Nd^{3+}) can absorb at 800 nm, a wavelength at which water has a low absorption coefficient. In these particles, Nd^{3+} is used as a sensitizer. It absorbs maximally at 800 nm, transferring energy to Yb^{3+} which subsequently transfers it to the activator ions (Tm^{3+}, Er^{3+}, etc.), resulting in UV or visible upconversion emission. These particles usually have a core–shell, or core with multiple shells structure to physically separate the sensitizer and activator ions such that deleterious energy transfer between the dopants does not quench the upconversion emission efficiency (Shen et al. 2013; Y.-F. Wang et al. 2013; Wen et al. 2013; Xie et al. 2013). These Nd^{3+}-doped UCNPs are relatively new and have not gone through extensive *in vitro* and *in vivo* testing. It remains to be seen whether their photoactivation capabilities are comparable to the UCNPs that have been used thus far.

Using host matrices different from the conventionally used $NaYF_4$ also produces UCNPs with excitation wavelengths different from 980 nm. For instance, when $BaSr_2Y_6O_{12}$ is used as the host matrix, the resulting nanoparticles can be excited at 1540 nm. Using $LiYF_4$ as a host matrix results in UCNPs with excitation at 1490 nm. Furthermore, these $LiYF_4$ UCNPs have a relatively high quantum yield (1.2% for 85 nm particles at 10–150 W cm^2).

Another hurdle that curbs the clinical potential of UCNPs is the uncertainty in terms of systemic toxicity, their clearance, and long-term effects on the body. Though their safety *in vitro* and in short-term *in vivo* studies has been extensively reported, their long-term toxicity effects and potential bioaccumulation are largely unexplored. Such studies exploring long-term effects need to be undertaken for these particles to enter into clinical practice. Besides these roadblocks, the lack of standardization owing to the existence of numerous synthesis methods makes it difficult to draw comparisons between resulting UCNPs. Quality control in terms of uniformity in particle size, optical properties, etc. also serves as an impediment in the scaling up of UCNP synthesis. These problems can be addressed to a large extent through standardization of synthesis techniques and increased automation. This would allow for greater consistency in the quality of the particles synthesized besides also enabling easy scaling up of the synthesis procedure, all of which are important for bringing these particles to commercial use.

9.7 Conclusion and Outlook

Technologies like upconversion overcome a major limitation associated with traditional photoactivation techniques, namely the use of low

penetrating or toxic UV/visible light for excitation by allowing the use of deeper penetrating and biologically friendly NIR light instead. This has made UCNPs nanotranducers of choice for phototherapeutic applications. These particles are excited by long-wavelength radiation (such as NIR) and can emit across a range of UV and visible light that can be tuned (depending on dopants and their ratios) in keeping with the absorption characteristics of the photoresponsive molecule in question. In the context of medicine, their unique properties like low autofluorescence, negligible photobleaching, tunability of emission peaks also enable simultaneous real time imaging, allowing one to track the delivery and distribution of therapeutic molecules that they carry.

Although promising, UCNPs do face certain limitations at present. Their quantum yield is low (<1%), thus a relatively high intensity of NIR is needed for activation, which may lead to potentially harmful heating effects owing to the high absorption of water at 970 nm, which is very close to the 980 nm light used to excite UCNPs. Efforts have been made to overcome some of these hurdles with innovations like the addition of an undoped shell such as $NaYF_4$ around the UCNPs to improve quantum yield, development of nanoparticles doped with neodymium ions that can be excited by 800 nm where the absorption coefficient of water is low, etc. Despite these efforts, UCNPs still have a long way to go before they can be put to clinical use. Batch-to-batch variability, uncertain systemic toxicity and clearance need to be addressed for their clinical and commercial potential to be realized.

References

Aebischer, A., M. Hostettler, J. Hauser, K. Krämer, T. Weber, H. U. Güdel, and H.-B. Bürgi. 2006. Structural and spectroscopic characterization of active sites in a family of light-emitting sodium lanthanide tetrafluorides. *Angew. Chem. Int. Ed.* 45 (17):2802–2806.

Allen, C. M., W. M. Sharman, and J. E. van Lier. 2001. Current status of phthalocyanines in the photodynamic therapy of cancer. *J. Porphyr. Phthalocya.* 5 (02):161–169.

Allison, R. R. and C. H. Sibata. 2008. Photofrin® photodynamic therapy: 2.0 mg/kg or not 2.0 mg/kg that is the question. *Photodiagnosis and Photodynamic Therapy* 5 (2):112–119.

Allison, R. R. and C. H. Sibata. 2010. Oncologic photodynamic therapy photosensitizers: A clinical review. *Photodiagnosis Photodyn. Ther.* 7 (2):61–75.

Ben-Hur, E. and I. Rosenthal. 1985. The phthalocyanines: A new class of mammalian cells photosensitizers with a potential for cancer phototherapy. *Int. J. Radiat. Biol. Relat. Stud. Phys. Chem. Med.* 47 (2):145–147.

Berg, K., A. Høgset, L. Prasmickaite et al. 2006. Photochemical internalization (PCI): A novel technology for activation of endocytosed therapeutic agents. *Med. Laser Appl.* 21 (4):239–250. doi: 10.1016/j.mla.2006.08.004.

Bernstein, Z. P., B. D. Wilson, A. R. Oseroff, C. M. Jones, S. E. Dozier, J. S. J. Brooks, R. Cheney, L. Foulke, T. S. Mang, and D. A. Bellnier. 1999. Photofrin photodynamic therapy for treatment of AIDS-related cutaneous Kaposi's sarcoma. *AIDS* 13 (13):1697–1704.

Berstad, M. B., A. Weyergang, and K. Berg. 2012. Photochemical internalization (PCI) of HER2-targeted toxins: Synergy is dependent on the treatment sequence. *Biochim. Biophys. Acta* 1820 (12):1849–1858. doi: 10.1016/j.bbagen.2012.08.027.

Boe, S., S. Saeboe-Larssen, and E. Hovig. 2010. Light-induced gene expression using messenger RNA molecules. *Oligonucleotides* 20 (1):1–6. doi: 10.1089/oli.2009.0209.

Bonnett, R. 1995. Photosensitizers of the porphyrin and phthalocyanine series for photodynamic therapy. *Chem. Soc. Rev.* 24 (1):19–33.

Boulnois, J.-L. 1986. Photophysical processes in recent medical laser developments: A review. *Laser. Med. Sci.* 1 (1):47–66.

Camerin, M., S. Rello, A. Villanueva, X. Ping, M. E. Kenney, M. A. J. Rodgers, and G. Jori. 2005. Photothermal sensitisation as a novel therapeutic approach for tumours: Studies at the cellular and animal level. *Eur. J. Cancer* 41 (8):1203–1212.

Carling, C.-J., F. Nourmohammadian, J.-C. Boyer, and N. R. Branda. 2010. Remote-control photorelease of caged compounds using near-infrared light and upconverting nanoparticles. *Angew. Chem. Int. Ed.* 49 (22):3782–3785.

Castano, A. P, P. Mroz, and M. R. Hamblin. 2006. Photodynamic therapy and anti-tumour immunity. *Nat. Rev. Cancer* 6 (7):535–545.

Chatterjee, D. K., M. K. Gnanasammandhan, and Y. Zhang. 2010. Small upconverting fluorescent nanoparticles for biomedical applications. *Small* 6 (24):2781–2795.

Chatterjee, D. K. and Z. Yong. 2008. Upconverting nanoparticles as nanotransducers for photodynamic therapy in cancer cells. *Nanomedicine (Future medicine)* 3(1): 73–82.

Cheng, L., C. Wang, and Z. Liu. 2013. Upconversion nanoparticles and their composite nanostructures for biomedical imaging and cancer therapy. *Nanoscale* 5 (1):23–37. doi: 10.1039/c2nr32311g.

Cheng, L., K. Yang, Y. Li, J. Chen, C. Wang, M. Shao, S.-T. Lee, and Z. Liu. 2011. Facile preparation of multifunctional upconversion nanoprobes for multimodal imaging and dual-targeted photothermal therapy. *Angew. Chem.* 123 (32):7523–7528.

Cheng, L., K. Yang, Y. Li, X. Zeng, M. Shao, S.-T. Lee, and Z. Liu. 2012. Multifunctional nanoparticles for upconversion luminescence/MR multimodal imaging and magnetically targeted photothermal therapy. *Biomaterials* 33 (7):2215–2222.

Cui, S., H. Chen, H. Zhu, J. Tian, X. Chi, Z. Qian, S. Achilefu, and Y. Gu. 2012a. Amphiphilic chitosan modified upconversion nanoparticles for in vivo photodynamic therapy induced by near-infrared light. *J. Mater. Chem.* 22 (11):4861–4873.

Cui, S., D. Yin, Y. Chen, Y. Di, H. Chen, Y. Ma, S. Achilefu, and Y. Gu. 2012b. *In vivo* targeted deep-tissue photodynamic therapy based on near-infrared light triggered upconversion nanoconstruct. *ACS Nano* 7 (1):676–688.

Dai, Y., H. Xiao, J. Liu, Q. Yuan, P. Ma, D. Yang, C. Li, Z. Cheng, Z. Hou, and P. Yang. 2013. *In vivo* multimodality imaging and cancer therapy by near-infrared light-triggered trans-platinum pro-drug-conjugated upconverison nanoparticles. *J. Am. Chem. Soc.* 135 (50):18920–18929.

Dominska, M. and D. M. Dykxhoorn. 2010. Breaking down the barriers: siRNA delivery and endosome escape. *J. Cell Sci.* 123 (8):1183–1189.

Dong, B., S. Xu, J. Sun, S. Bi, D. Li, X. Bai, Y. Wang, L. Wang, and H. Song. 2011. Multifunctional $NaYF_4$: Yb3+, Er3+@ Ag core/shell nanocomposites: Integration of upconversion imaging and photothermal therapy. *J. Mater. Chem.* 21 (17):6193–6200.

Dougherty, T. J., C. J. Gomer, B. W. Henderson, G. Jori, D. Kessel, M. Korbelik, J. Moan, and Q. Peng. 1998. Photodynamic therapy. *J. Natl. Cancer Inst.* 90 (12):889–905.

Fan, W., B. Shen, W. Bu, F. Chen, Q. He, K. Zhao, S. Zhang, L. Zhou, W. Peng, and Q. Xiao. 2014. A smart upconversion-based mesoporous silica nanotheranostic system for synergetic chemo-/radio-/photodynamic therapy and simultaneous MR/UCL imaging. *Biomaterials* 35 (32):8992–9002.

Fretz, M. M., A. Hogset, G. A. Koning, W. Jiskoot, and G. Storm. 2007. Cytosolic delivery of liposomally targeted proteins induced by photochemical internalization. *Pharm. Res.* 24 (11):2040–2047. doi: 10.1007/s11095-007-9338-9.

Garcia, J. V., J. Yang, D. Shen, C. Yao, X. Li, R. Wang, G. D. Stucky, D. Zhao, P. C. Ford, and F. Zhang. 2012. NIR-triggered release of caged nitric oxide using upconverting nanostructured materials. *Small* 8 (24):3800–3805.

Gillmeister, M. P., M. J. Betenbaugh, and P. S. Fishman. 2011. Cellular trafficking and photochemical internalization of cell penetrating peptide linked cargo proteins: A dual fluorescent labeling study. *Bioconjug. Chem.* 22 (4):556–566. doi: 10.1021/bc900445g.

Guo, H., H. Qian, N. M. Idris, and Y. Zhang. 2010. Singlet oxygen-induced apoptosis of cancer cells using upconversion fluorescent nanoparticles as a carrier of photosensitizer. *Nanomed. Nanotechnol. Biol. Med.* 6 (3):486–495.

Heer, S., K. Kömpe, H.-U. Güdel, and M. Haase. 2004. Highly efficient multicolour upconversion emission in transparent colloids of lanthanide-doped $NaYF_4$ nanocrystals. *Adv. Mater.* 16 (23–24):2102–2105.

Henderson, B. W. and T. J. Dougherty. 1992. How does photodynamic therapy work? *Photochem. Photobiol.* 55 (1):145–157.

Henderson, B. W. and V. H. Fingar. 1987. Relationship of tumor hypoxia and response to photodynamic treatment in an experimental mouse tumor. *Cancer Res.* 47 (12):3110–3114.

Hou, Z., Y. Zhang, K. Deng, Y. Chen, X. Li, X. Deng, Z. Cheng, H. Lian, C. Li, and J. Lin. 2015. UV-emitting upconversion-based TiO_2 photosensitizing nanoplatform: Near-infrared light mediated *in vivo* photodynamic therapy via mitochondria-involved apoptosis pathway. *ACS Nano* 9 (3):2584–2599.

Hu, M., J. Chen, Z. Y. Li, L. Au, G. V. Hartland, X. Li, M. Marquez, and Y. Xia. 2006. Gold nanostructures: Engineering their plasmonic properties for biomedical applications. *Chem. Soc. Rev.* 35 (11):1084–1094. doi: 10.1039/b517615h.

Huang, X., P. K. Jain, I. H. El-Sayed, and M. A. El-Sayed. 2008. Plasmonic photothermal therapy (PPTT) using gold nanoparticles. *Laser. Med. Sci.* 23 (3):217–228.

Idris, N. M., M. K. Gnanasammandhan, J. Zhang, P. C. Ho, R. Mahendran, and Y. Zhang. 2012. *In vivo* photodynamic therapy using upconversion nanoparticles as remote-controlled nanotransducers. *Nat. Med.* 18 (10):1580–1585. http://www.nature.com/nm/journal/v18/n10/abs/nm.2933.html#supplementary-information.

Idris, N. M., M. K. G. Jayakumar, A. Bansal, and Y. Zhang. 2015. Upconversion nanoparticles as versatile light nanotransducers for photoactivation applications. *Chem. Soc. Rev.* 44(6): 1449–1478.

Idris, N. M., S. S. Lucky, Z. Li, K. Huang, and Y. Zhang. 2014. Photoactivation of core–shell titania coated upconversion nanoparticles and their effect on cell death. *J. Mater. Chem. B* 2 (40):7017–7026.

Jayakumar, M. K. G., A. Bansal, K. Huang, R. Yao, B. N. Li, and Y. Zhang. 2014. Near-infrared-light-based nano-platform boosts endosomal escape and controls gene knockdown *in vivo*. *ACS Nano* 8(5):4848–4858.

Jayakumar, M. K., N. M. Idris, and Y. Zhang. 2012. Remote activation of biomolecules in deep tissues using near-infrared-to-UV upconversion nanotransducers. *Proc. Natl. Acad. Sci. USA* 109 (22):8483–8488. doi: 10.1073/pnas.1114551109.

Jin, C. S., J. F. Lovell, J. Chen, and G. Zheng. 2013. Ablation of hypoxic tumors with dose-equivalent photothermal, but not photodynamic, therapy using a nanostructured porphyrin assembly. *ACS Nano* 7 (3):2541–2550.

Jin, H., J. F. Lovell, J. Chen, K. Ng, W. Cao, L. Ding, Z. Zhang, and G. Zheng. 2011. Cytosolic delivery of LDL nanoparticle cargo using photochemical internalization. *Photochem. Photobiol. Sci.* 10 (5):810–816. doi: 10.1039/c0pp00350f.

Jin, S., L. Zhou, Z. Gu, G. Tian, L. Yan, W. Ren, W. Yin, X. Liu, X. Zhang, and Z. Hu. 2013. A new near infrared photosensitizing nanoplatform containing blue-emitting up-conversion nanoparticles and hypocrellin A for photodynamic therapy of cancer cells. *Nanoscale* 5 (23):11910–11918.

Juzeniene, A., Q. Peng, and J. Moan. 2007. Milestones in the development of photodynamic therapy and fluorescence diagnosis. *Photochem. Photobiol. Sci.* 6 (12):1234–1245.

Krämer, K. W., D. Biner, G. Frei, H. U. Güdel, M. P. Hehlen, and S. R. Lüthi. 2004. Hexagonal sodium yttrium fluoride based green and blue emitting upconversion phosphors. *Chem. Mater.* 16 (7):1244–1251.

Lilletvedt, M., H. H. Tonnesen, A. Hogset, S. A. Sande, and S. Kristensen. 2011. Evaluation of physicochemical properties and aggregation of the photosensitizers TPCS2a and TPPS2a in aqueous media. *Die Pharmazie Int. J. Pharm. Sci.* 66 (5):325–333.

Liu, J., W. Bu, L. Pan, and J. Shi. 2013. NIR-triggered anticancer drug delivery by upconverting nanoparticles with integrated azobenzene-modified mesoporous silica. *Angew. Chem. Int. Ed.* 52(16):4375–4379.

Liu, K., X. Liu, Q. Zeng, Y. Zhang, L. Tu, T. Liu, X. Kong, Y. Wang, F. Cao, and S. A. G. Lambrechts. 2012. Covalently assembled NIR nanoplatform for simultaneous fluorescence imaging and photodynamic therapy of cancer cells. *ACS Nano* 6 (5):4054–4062.

Liu, Q., Y. Sun, T. Yang, W. Feng, C. Li, and F. Li. 2011. Sub-10 nm hexagonal lanthanide-doped $NaLuF_4$ upconversion nanocrystals for sensitive bioimaging *in vivo*. *J. Am. Chem. Soc.* 133 (43):17122–17125.

Liu, X., C. N. Kim, J. Yang, R. Jemmerson, and X. Wang. 1996. Induction of apoptotic program in cell-free extracts: Requirement for dATP and cytochrome c. *Cell* 86 (1):147–157.

Liu, X., M. Zheng, X. Kong, Y. Zhang, Q. Zeng, Z. Sun, W. J. Buma, and H. Zhang. 2013. Separately doped upconversion-C 60 nanoplatform for NIR imaging-guided photodynamic therapy of cancer cells. *Chem. Commun.* 49 (31):3224–3226.

Lucky, S. S., N. M. Idris, Z. Li, K. Huang, K. C. Soo, and Y. Zhang. 2015. Titania coated upconversion nanoparticles for near-infrared light triggered photodynamic therapy. *ACS Nano* 9 (1):191–205.

Mitchell, J. B., S. McPherson, W. DeGraff, J. Gamson, A. Zabell, and A. Russo. 1985. Oxygen dependence of hematoporphyrin derivative-induced photoinactivation of Chinese hamster cells. *Cancer Res.* 45 (5):2008–2011.

Nakamura, T., A. Tamura, H. Murotani, M. Oishi, Y. Jinji, K. Matsuishi, and Y. Nagasaki. 2010. Large payloads of gold nanoparticles into the polyamine network core of stimuli-responsive PEGylated nanogels for selective and non-invasive cancer photothermal therapy. *Nanoscale* 2 (5):739–746.

Ni, D., J. Zhang, W. Bu, H. Xing, F. Han, Q. Xiao, Z. Yao, F. Chen, Q. He, and J. Liu. 2014. Dual-targeting upconversion nanoprobes across the blood–brain barrier for magnetic resonance/fluorescence imaging of intracranial glioblastoma. *ACS Nano* 8 (2):1231–1242.

Nikfarjam, M., V. Muralidharan, and C. Christophi. 2005. Mechanisms of focal heat destruction of liver tumors. *J. Surg. Res.* 127 (2):208–223.

Nishiyama, N., A. Iriyama, W. D. Jang et al. 2005. Light-induced gene transfer from packaged DNA enveloped in a dendrimeric photosensitizer. *Nat. Mater.* 4 (12):934–41. doi: 10.1038/nmat1524.

O'Connell, M. J., S. M. Bachilo, C. B. Huffman, V. C. Moore, M. S. Strano, E. H. Haroz, K. L. Rialon, P. J. Boul, W. H. Noon, and C. Kittrell. 2002. Band gap fluorescence from individual single-walled carbon nanotubes. *Science* 297 (5581):593–596.

Oliveira, S., M. M. Fretz, A. Hogset, G. Storm, and R. M. Schiffelers. 2007. Photochemical internalization enhances silencing of epidermal growth factor receptor through improved endosomal escape of siRNA. *Biochim. Biophys. Acta* 1768 (5):1211–1217. doi: 10.1016/j.bbamem.2007.01.013.

Ouyang, J., D. Yin, X. Cao, C. Wang, K. Song, B. Liu, L. Zhang, Y. Han, and M. Wu. 2014. Synthesis of $NaLuF_4$-based nanocrystals and large enhancement of upconversion luminescence of $NaLuF_4$: Gd, Yb, Er by coating an active shell for bioimaging. *Dalton Trans.* 43 (37):14001–14008.

Park, Y. I., H. M. Kim, J. H. Kim, K. C. Moon, B. Yoo, K. T. Lee, N. Lee, Y. Choi, W. Park, and D. Ling. 2012. Theranostic probe based on lanthanide-doped nanoparticles for simultaneous *in vivo* dual-modal imaging and photodynamic therapy. *Adv. Mater.* 24 (42):5755–5761.

Pelliccioli, A. P. and J. Wirz. 2002. Photoremovable protecting groups: Reaction mechanisms and applications. *Photochem.Photobiol. Sci.* 1 (7):441–458. doi: 10.1039/b200777k.

Peng, Q., K. Berg, J. Moan, M. Kongshaug, and J. M. Nesland. 1997. 5-Aminolevulinic acid-based photodynamic therapy: Principles and experimental research. *Photochem. Photobiol.* 65 (2):235–251.

Plaetzer, K., B. Krammer, J. Berlanda, F. Berr, and T. Kiesslich. 2009. Photophysics and photochemistry of photodynamic therapy: Fundamental aspects. *Laser. Med. Sci.* 24 (2):259–268.

Qian, H. S., H. C. Guo, P. C.-L. Ho, R. Mahendran, and Y. Zhang. 2009. Mesoporous-silica-coated up-conversion fluorescent nanoparticles for photodynamic therapy. *Small* 5 (20):2285–2290.

Qian, L. P., L. H. Zhou, H.-P. Too, and G.-M. Chow. 2011. Gold decorated $NaYF_4$: Yb, Er/$NaYF_4$/silica (core/shell/shell) upconversion nanoparticles for photothermal destruction of BE (2)-C neuroblastoma cells. *J. Nanopart. Res.* 13 (2):499–510.

Qiao, X.-F., J.-C. Zhou, J.-W. Xiao, Y.-F. Wang, L.-D. Sun, and C.-H. Yan. 2012. Triple-functional core–shell structured upconversion luminescent nanoparticles covalently grafted with photosensitizer for luminescent, magnetic resonance imaging and photodynamic therapy *in vitro*. *Nanoscale* 4 (15):4611–4623.

See, K. L., I. J. Forbes, and W. H. Betts. 1984. Oxygen dependency of photocytotoxicity with haematoporphyrin derivative. *Photochem. Photobiol.* 39 (5):631–634.

Selbo, P. K., A. Weyergang, A. Bonsted, S. G. Bown, and K. Berg. 2006. Photochemical internalization of therapeutic macromolecular agents: A novel strategy to kill multidrug-resistant cancer cells. *J. Pharmacol. Exp. Ther.* 319 (2):604–612. doi: 10.1124/jpet.106.109165.

Shen, J., G. Chen, A.-M. Vu, W. Fan, O. S. Bilsel, C.-C. Chang, and G. Han. 2013. Engineering the upconversion nanoparticle excitation wavelength: Cascade sensitization of tri-doped upconversion colloidal nanoparticles at 800 nm. *Adv. Opt. Mater.* 1 (9):644–650.

Shieh, Y.-A., S.-J. Yang, M.-F. Wei, and M.-J. Shieh. 2010. Aptamer-based tumor-targeted drug delivery for photodynamic therapy. *ACS Nano* 4 (3):1433–1442.

Sortino, S. 2012. Photoactivated nanomaterials for biomedical release applications. *J. Mater. Chem.* 22 (2):301. doi: 10.1039/c1jm13288a.

Tan, W., M. J Donovan, and J. Jiang. 2013. Aptamers from cell-based selection for bioanalytical applications. *Chem. Rev.* 113 (4):2842–2862.

Ungun, B., R. K. Prud'Homme, S. J. Budijon, J. Shan, S. F. Lim, Y. Ju, and R. Austin. 2009. Nanofabricated upconversion nanoparticles for photodynamic therapy. *Opt. Express* 17 (1):80–86.

Wang, C., L. Cheng, Y. Liu, X. Wang, X. Ma, Z. Deng, Y. Li, and Z. Liu. 2013. Imaging-guided pH-sensitive photodynamic therapy using charge reversible upconversion nanoparticles under near-infrared light. *Adv. Funct. Mater.* 23 (24):3077–3086.

Wang, C., H. Tao, L. Cheng, and Z. Liu. 2011. Near-infrared light induced *in vivo* photodynamic therapy of cancer based on upconversion nanoparticles. *Biomaterials* 32 (26):6145–6154.

Wang, C., D. Yin, K. Song, J. Ouyang, and B. Liu. 2014. Preparation of bi-functional $NaGdF_4$-based upconversion nanocrystals and fine-tuning of emission colors of the nanocrystals by doping with Mn^{2+}. *Vacuum* 107:311–315.

Wang, H. J., R. Shrestha, and Y. Zhang. 2014. Encapsulation of photosensitizers and upconversion nanocrystals in lipid micelles for photodynamic therapy. *Part. Part. Syst. Char.* 31 (2):228–235.

Wang, Xin, K. Liu, G. Yang, L. Cheng, L. He, Y. Liu, Y. Li, L. Guo, and Z. Liu. 2014. Near-infrared light triggered photodynamic therapy in combination with gene therapy using upconversion nanoparticles for effective cancer cell killing. *Nanoscale* 6 (15):9198–9205.

Wang, Xu, C.-X. Yang, J.-T. Chen, and X.-P. Yan. 2014. A dual-targeting upconversion nanoplatform for two-color fluorescence imaging-guided photodynamic therapy. *Anal. Chem.* 86 (7):3263–3267.

Wang, Y., H. Wang, D. Liu, S. Song, X. Wang, and H. Zhang. 2013. Graphene oxide covalently grafted upconversion nanoparticles for combined NIR mediated imaging and photothermal/photodynamic cancer therapy. *Biomaterials* 34 (31):7715–7724.

Wang, Y.-F., G.-Y. Liu, L.-D. Sun, J.-W. Xiao, J.-C. Zhou, and C.-H. Yan. 2013. Nd^{3+}-sensitized upconversion nanophosphors: Efficient *in vivo* bioimaging probes with minimized heating effect. *ACS Nano* 7 (8):7200–7206.

Wen, H., H. Zhu, X. Chen, T. F. Hung, B. Wang, G. Zhu, S. F. Yu, and F. Wang. 2013. Upconverting near-infrared light through energy management in core–shell–shell nanoparticles. *Angew. Chem.* 125 (50):13661–13665.

Xie, X., N. Gao, R. Deng, Q. Sun, Q.-H. Xu, and X. Liu. 2013. Mechanistic investigation of photon upconversion in Nd^{3+}-sensitized core–shell nanoparticles. *J. Am. Chem. Soc.* 135 (34):12608–12611.

Yan, B., J.-C. Boyer, N. R. Branda, and Y. Zhao. 2011. Near-infrared light-triggered dissociation of block copolymer micelles using upconverting nanoparticles. *J. Am. Chem. Soc.* 133 (49):19714–19717.

Yan, B., J.-C. Boyer, D. Habault, N. R. Branda, and Y. Zhao. 2012. Near infrared light triggered release of biomacromolecules from hydrogels loaded with upconversion nanoparticles. *J. Am. Chem. Soc.* 134 (40):16558–16561.

Yang, Y., F. Liu, X. Liu, and B. Xing. 2013a. NIR light controlled photorelease of siRNA and its targeted intracellular delivery based on upconversion nanoparticles. *Nanoscale* 5 (1):231–238. doi: 10.1039/c2nr32835f.

Yang, Y., B. Velmurugan, X. Liu, and B. Xing. 2013b. NIR photoresponsive crosslinked upconverting nanocarriers toward selective intracellular drug release. *Small* 9(17):2937–2944.

Yu, H., J. Li, D. Wu, Z. Qiu, and Y. Zhang. 2010. Chemistry and biological applications of photo-labile organic molecules. *Chem. Soc. Rev.* 39 (2):464–473. doi: 10.1039/b901255a.

Yuan, Y., Y. Min, Q. Hu, B. Xing, and B. Liu. 2014. NIR photoregulated chemo- and photodynamic cancer therapy based on conjugated polyelectrolyte–drug conjugate encapsulated upconversion nanoparticles. *Nanoscale* 6 (19):11259–11272.

Zhang, P., W. Steelant, M. Kumar, and M. Scholfield. 2007. Versatile photosensitizers for photodynamic therapy at infrared excitation. *J. Am. Chem. Soc.* 129 (15):4526–4527.

Zhao, L., J. Peng, Q. Huang, C. Li, M. Chen, Y. Sun, Q. Lin, L. Zhu, and F. Li. 2013. Near-infrared photoregulated drug release in living tumor tissue via yolk–shell upconversion nanocages. *Adv. Funct. Mat.* 24(3):363–371. doi: 10.1002/adfm.201302133.

Zhao, Z., Y. Han, C. Lin, D. Hu, F. Wang, X. Chen, Z. Chen, and N. Zheng. 2012. Multifunctional core–shell upconverting nanoparticles for imaging and photodynamic therapy of liver cancer cells. *Chem. Asian J.* 7 (4):830–837.

Zhou, A., Y. Wei, B. Wu, Q. Chen, and D. Xing. 2012. Pyropheophorbide A and c(RGDyK) comodified chitosan-wrapped upconversion nanoparticle for targeted near-infrared photodynamic therapy. *Mol. Pharmaceut.* 9 (6):1580–1589.